Application of heavy-quark effective theory to lattice QCD. II. Radiative corrections to heavy-light currents

Junpei Harada,[1] Shoji Hashimoto,[2] Ken-Ichi Ishikawa,[2,3] Andreas S. Kronfeld,[3,4] Tetsuya Onogi,[1,5,*] and Norikazu Yamada[2]
[1]*Department of Physics, Hiroshima University, Higashi-Hiroshima 739-8526, Japan*
[2]*High Energy Accelerator Research Organization (KEK), Tsukuba 305-0801, Japan*
[3]*Center for Computational Physics, University of Tsukuba, Tsukuba 305-8577, Japan*
[4]*Theoretical Physics Department, Fermi National Accelerator Laboratory, Batavia, Illinois 60510*
[5]*Yukawa Institute for Theoretical Physics, Kyoto University, Sakyo-ku, Kyoto 606-8502, Japan*
(Received 20 December 2001; published 16 May 2002)

We apply heavy-quark effective theory to separate long- and short-distance effects of heavy quarks in lattice gauge theory. In this approach, the inverse heavy-quark mass and the lattice spacing are treated as short distances, and their effects are lumped into short-distance coefficients. We show how to use this formalism to match lattice gauge theory to continuum QCD, order by order in the heavy-quark expansion. In this paper, we focus on heavy-light currents. In particular, we obtain one-loop results for the matching factors of lattice currents, needed for heavy-quark phenomenology, such as the calculation of heavy-light decay constants, and heavy-to-light transition form factors. Results for the Brodsky-Lepage-Mackenzie scale q^* are also given.

DOI: 10.1103/PhysRevD.65.094513 PACS number(s): 12.38.Gc, 12.15.Hh, 13.20.He

I. INTRODUCTION

A key ingredient in flavor physics is the calculation of hadronic matrix elements of the electroweak Hamiltonian. For example, one would like to calculate, from first principles, quantities such as leptonic decay constants, semileptonic form factors, and the amplitudes for neutral-meson mixing. Numerical calculations with lattice QCD offer a way to obtain these quantities, eventually with well-controlled estimates of the numerical uncertainties [1].

The properties of B and D mesons are especially interesting, but the relatively large b and c quark masses make it difficult, with today's computers, to carry out lattice calculations in the limit $m_Q a \to 0$ for which lattice QCD was first developed. (Here m_Q is the b or c quark mass, and a is the lattice spacing.) One can, however, use the simplifying features of the heavy-quark limit of QCD to make lattice calculations tractable. As m_Q is increased far above the typical scale of the wave function, $\Lambda_{\rm QCD}$, the hadrons' wave functions depend less and less on m_Q. As $m_Q \to \infty$ the wave functions become flavor and spin symmetric [2]. For quarkonia similar simplifications occur, including spin symmetry [3].

In this paper we construct vector and axial vector currents with one quark heavy and the other light. These currents are needed to obtain the decay constants of heavy-light mesons, and the form factors for decays of the form $H \to L l \nu_l$, where H is a charmed or b-flavored hadron (e.g., $B,D;\Lambda_b,\Lambda_c$), decaying to a light hadron L (e.g., π, K, ρ; p, etc.) and a lepton l and its neutrino ν_l. In particular, we provide a way to treat radiative and power corrections consistently. This paper is a sequel to Ref. [4], which focussed on power corrections. Here we discuss the case of heavy-light bilinears in detail, and we compute explicitly the matching factors for the currents introduced in the ''Fermilab'' formalism [5]. Heavy-heavy bilinears are considered in a companion paper [6].

To interpret lattice calculations when $m_Q a \ll 1$, it is convenient to describe cutoff effects with the Symanzik local effective Lagrangian (LE$\mathcal{L}$) and expand the LE$\mathcal{L}$'s short-distance coefficients in powers of $m_Q a$ [7–10]. When $m_Q a \not\ll 1$, however, one should realize that it is not lattice gauge theory that breaks down but rather the Symanzik description, especially its expansion in $m_Q a$. If $m_Q a$ is large because $m_Q \gg \Lambda_{\rm QCD}$, then the simplifying features of the heavy-quark limit provide an alternative. Instead of matching lattice gauge theory directly to continuum QCD, one can match to the heavy-quark effective theory (HQET) or, for quarkonia, to nonrelativistic QCD (NRQCD). In this approach, the inverse heavy-quark mass and the lattice spacing are both treated as short distances, and a simple picture arises, in which heavy-quark discretization effects are lumped into short-distance coefficients. Heavy-quark cutoff effects are systematically reducible, by adjusting the heavy-quark expansion for lattice gauge theory to agree term-by-term with continuum QCD.

Such application of HQET to lattice QCD was started in Ref. [4], building on Ref. [5]. In this paper we extend the formalism to heavy-light currents. We use the heavy-quark expansion, as generated by HQET, to derive matching conditions, which are valid for all $m_Q a$ and to all orders in the gauge coupling. Our derivation is explicit for dimension-four currents, which is the next-to-leading dimension, but generalization to higher-dimension operators should be clear.

We also present explicit results for the one-loop radiative corrections to the normalization of the current. These calculations show that the temporal and spatial components of the current do not have the same radiative corrections. This feature has been found already [11,12], and the HQET formalism shows why it arises. In deriving these results we have found a compact way of arranging the Dirac algebra, which

*Present address: Yukawa Institute, Kyoto University, Kyoto, Japan.

may be useful for calculations with actions, such as highly improved actions, that are not considered here.

As expected, the coefficients have a strong mass dependence. Most of this dependence can be handled nonperturbatively [13–15]. For equal mass, it is simple to normalize the temporal vector current, for all masses. One can then form ratios of renormalization factors, from which the dominant mass dependence drops out. Results for these combinations are also presented, in Sec. IV.

Our one-loop results extend those of Ref. [12], which considered heavy-light currents with the Sheikholeslami-Wohlert (SW) action [16] for Wilson fermions [17] and also with non-relativistic QCD (NRQCD). Results for the Wilson action [17] have been obtained first by Kuramashi [11]. In Refs. [11,12] a term in the currents, the so-called rotation term [18,5], which is needed for tree-level improvement at order $1/m_Q$, was omitted. Here we include the rotation, obtaining the algebraic expression of the Feynman diagrams for the full Fermilab action. We present numerical results for the Wilson action (without rotation) and the SW action (with and without rotation). These results are appropriate for recent calculations of decay constants [19–23], which used the radiative corrections calculated in Refs. [11,12]. Our new results have been used in a recent calculation of the form factors for the decays $B\to\pi l\nu_l$ and $D\to\pi l\nu_l$ [15]. We also have obtained results for the Fermilab action on anisotropic lattices [24].

Our formalism should be useful for computing matching factors (beyond one-loop) also in lattice NRQCD [25]. Applied to the static limit [26], it generalizes the formalism of Eichten and Hill [27]. At one-loop order, similar methods have been developed to calculate the heavy-light matching coefficients for lattice NRQCD [28,29]. As in the Symanzik program [7–9], the advantage of introducing a continuum effective field theory is that the formalism provides a clear definition of the matching coefficients at every order in perturbation theory (in the gauge coupling). Indeed, it may also provide a foundation for a non-perturbative improvement program.

This paper is organized as follows. Section II discusses three ways to separate long and short distance physics with (continuum) effective field theories. The first is Symanzik's description of lattice spacing effects; we also discuss its breakdown when $m_Q a \not\ll 1$. The second is the HQET description of heavy quarks, applied to continuum QCD. The third is the HQET description of heavy quarks on the lattice, which applies when $m_Q \gg \Lambda_{\rm QCD}$, for all $m_Q a$. In particular, we obtain a definition of the matching factors for the vector and axial-vector heavy-light currents. Section II also shows how the HQET matching procedure is related to the Symanzik procedure in the regime where both apply. Then, the Fermilab action is reviewed in Sec. III, and in Sec. IV we present one-loop results for the matching factors. Some concluding remarks are made in Sec. V. Three Appendixes contain details of the one-loop calculation, including an outline of a method to obtain compact expressions, and explicit results for the one-loop Feynman integrands for the renormalization factors with the full Fermilab action.

Instead of printing tables of the numerical results in Sec. IV, we are making a suite of programs freely available [30]. This suite includes programs for the heavy-heavy currents treated in our companion paper [6].

II. MATCHING TO CONTINUUM FIELD THEORIES

In this section we discuss how to interpret the physical content of lattice field theories by matching to continuum field theories. First, the standard Symanzik formalism for describing cutoff effects is reviewed, and we recall how this description breaks down for heavy quarks. After reviewing the HQET description of (continuum) QCD, we adapt HQET to describe lattice gauge theory. Comparison of the two then yields a matching procedure that is valid whenever $m_Q \gg \Lambda_{\rm QCD}$, and for all $m_Q a$. In the limit $m_Q a \ll 1$ both the HQET and the Symanzik descriptions should apply, so we are able to derive relations between some of the matching coefficients.

A. Symanzik formalism

The customary way to define matching factors for lattice gauge theory is to apply Symanzik's formalism. Then the short-distance lattice artifacts are described by a local effective Lagrangian (LE$\mathcal{L}$) and local effective operators. For the Lagrangian of any lattice field theory one can write [7,8]

$$\mathcal{L}_{\rm lat} \doteq \mathcal{L}_{\rm Sym}, \tag{2.1}$$

where the symbol $\doteq$ can be read "has the same on-shell matrix elements as." The left-hand side is a lattice field theory, and the right-hand side is a continuum field theory, whose ultraviolet behavior is regulated and renormalized completely separately from the lattice of the left-hand side. The LE$\mathcal{L}$ is the Lagrangian of the corresponding continuum field theory, plus extra terms to describe discretization effects. For lattice QCD

$$\mathcal{L}_{\rm Sym} = \mathcal{L}_{\rm QCD} + \mathcal{L}_I, \tag{2.2}$$

where $\mathcal{L}_{\rm QCD}$ is the renormalized, continuum QCD Lagrangian. We focus on the quarks, so for our purposes

$$\mathcal{L}_{\rm QCD} = -\bar{q}(\not{D} + m_q)q. \tag{2.3}$$

Lattice artifacts are described by higher-dimension operators,

$$\mathcal{L}_I = aK_{\sigma\cdot F}\bar{q}i\sigma_{\mu\nu}F^{\mu\nu}q + \cdots, \tag{2.4}$$

where a is the lattice spacing and $K_{\sigma\cdot F}$ is a short-distance coefficient that depends on details of the lattice action [9]. The lattice artifacts in $\mathcal{L}_I$ can be treated as a perturbation. In this way a series can be developed, with matrix elements in the (continuum) eigenstates of $\mathcal{L}_{\rm QCD}$. Equation (2.2) omits dimension-five operators of the form $\bar{q}R(\not{D} + m_q)q$ or $\bar{q}(-\overleftarrow{\not{D}} + m_q)Rq$, for arbitrary R, which make no contribution to on-shell matrix elements, owing to the equations of motion implied by Eq. (2.3).

The vector and axial vector currents can be described in a similar way. Consider, for example, the flavor-changing transition $s \to u$. Then one may write [9]

$$V^{\mu}_{\rm lat} \doteq Z_V^{-1} \mathcal{V}^{\mu} - a K_V \partial_{\nu} \overline{u} \sigma^{\mu\nu} s + \cdots, \tag{2.5}$$

$$A^{\mu}_{\rm lat} \doteq Z_A^{-1} \mathcal{A}^{\mu} + a K_A \partial^{\mu} \overline{u} i \gamma_5 s + \cdots, \tag{2.6}$$

where

$$\mathcal{V}^{\mu} \equiv \overline{u} i \gamma^{\mu} s, \tag{2.7}$$

$$\mathcal{A}^{\mu} \equiv \overline{u} i \gamma^{\mu} \gamma_5 s, \tag{2.8}$$

are the vector and axial vector currents in QCD. Further dimension-four operators are omitted, because they are linear combinations of those listed and others that vanish by the equations of motion. Like the terms of dimension five and higher in $\mathcal{L}_I$, the dimension-four currents can be treated as perturbations. Matrix elements of $Z_V V^{\mu}_{\rm lat}$ and $Z_A A^{\mu}_{\rm lat}$ then give those of continuum QCD, at least in the limit $a \to 0$.

The short-distance coefficients—$K_{\sigma\cdot F}$, K_J, and Z_J ($J = V,A$)—are, in general, functions of the gauge coupling and the quark masses (in lattice units), and they depend on the renormalization scheme of the LE$\mathcal{L}$. For $m_q a \ll 1$ ($q = u,d,s$), it is consistent and satisfactory to replace $K_{\sigma\cdot F}$ and K_J with their values at $m_q a = 0$, and to replace the Z_J with the first two terms of the Taylor expansion around $m_q a = 0$. For example, with Wilson fermions [17,16] and conventional bilinears for the lattice currents, one finds $K_V^{[0]} = K_A^{[0]} = 0$, and

$$K^{[0]}_{\sigma\cdot F} = \tfrac{1}{4}(1 - c_{\rm SW}) + O(ma), \tag{2.9}$$

$$Z_V^{[0]} = Z_A^{[0]} = 1 + \tfrac{1}{2}(m_u + m_s)a + O(m^2 a^2), \tag{2.10}$$

where the superscript "[0]" denotes the tree level, and $c_{\rm SW}$ is the clover coupling of the SW action [16] (cf. Sec. III). Moreover, in the hands of the *Alpha* Collaboration [9,10], Eqs. (2.1)–(2.6) are the foundation of a non-perturbative procedure for adjusting $K_{\sigma\cdot F}$, K_V, and K_A to be of order aM_p, where M_p is a (light) hadronic mass scale, and also for computing Z_V and Z_A non-perturbatively (through order $M_p a$). Then all lattice artifacts in the mass spectrum, decay constants, and form factors are of order a^2.

For a heavy flavor Q, however, it is not practical to keep $m_Q a$ small enough so that this program straightforwardly applies. Recent work that uses the fully $O(a)$-improved action and currents has chosen the heavy-quark mass $m_Q a$ to be as large as 0.7 or so. Thus, $(m_Q a)^2$ is not small,[1] and one should check whether contributions of order $(m_Q a)^2$ are under control. Indeed, if one keeps the full mass dependence in the coefficients, one finds that the simple description of Eqs. (2.2)–(2.6) breaks down. The relation between energy and momentum becomes [5,31]

$$E^2(\boldsymbol{p}) = m_1^2 + \frac{m_1}{m_2}\boldsymbol{p}^2 + O(p^4 a^2), \tag{2.11}$$

where, for the Wilson and SW actions,

$$m_1^{[0]} a = \ln(1 + m_0 a), \tag{2.12}$$

$$\frac{1}{m_2^{[0]} a} = \frac{2}{m_0 a (2 + m_0 a)} + \frac{1}{1 + m_0 a}, \tag{2.13}$$

and m_0 is the bare lattice mass. Generalizations valid at every order in perturbation theory also have been derived [31]. In a similar vein, the spatial and temporal components of the currents no longer take the same matching coefficients, as shown by explicit one-loop calculations [11,12].

The energy-momentum relation in Eq. (2.11) is obtained for $\boldsymbol{p}a \ll 1$ but $m_Q a \not\ll 1$. It can be described by modifying the standard LE$\mathcal{L}$ to

$$\mathcal{L}_{\rm lat} \doteq -\overline{q}\left(\gamma_4 D_4 + \sqrt{\frac{m_1}{m_2}}\boldsymbol{\gamma}\cdot\boldsymbol{D} + m_1 \right) q + \mathcal{L}_I', \tag{2.14}$$

that is, temporal and spatial directions must be treated asymmetrically in the dimension-four Lagrangian, and also in the higher-dimension terms $\mathcal{L}_I'$. From the tree-level formulas, Eqs. (2.12) and (2.13),

$$\frac{m_1}{m_2} = 1 - \tfrac{2}{3} m_1^2 a^2 + \tfrac{1}{2} m_1^3 a^3 + \cdots, \tag{2.15}$$

so one sees that the deviation from the standard description is of order $(ma)^2$. [At the one-loop order [31], and at every order in g^2, Eq. (2.15) still has no term linear in ma.] One can arrive at Eqs. (2.14) and (2.15) also by starting with Eq. (2.2), including higher-dimension terms, and eliminating $\gamma_4 D_4^3$ and D_4^4, etc., by applying the equations of motion.

In any case, deviations of m_1/m_2—and similar ratios—from 1 are present in lattice calculations. With the Wilson or SW actions $1 - m_1/m_2$, for example, is 10% or greater for $m_1 a > 0.6$. Although this numerical estimate is made at the tree level, it is implausible that radiative corrections or bound-state effects could wash the error away. In summary, the description of Eqs. (2.2)–(2.6) is no longer accurate when $m_Q a \not\ll 1$.

There are several possible remedies. One is to do numerical calculations with a so small that, even for the b quark, $m_b a \ll 1$. Despite the exponential growth in computer power, this remedy will not be available for many years. Another remedy is to add a parameter to the lattice action, which can be tuned to set $m_1 = m_2$ [5]. An example of this is an action with two hopping parameters. Then, the continuum description can again take the form in Eq. (2.2), starting with the continuum $\mathcal{L}_{\rm QCD}$, although it is still useful to describe the higher-dimension terms asymmetrically. A third remedy is to realize that it is the *description*, rather than the underlying lattice gauge theory, that has broken down. Since lattice gauge theory with Wilson fermions has a well-behaved heavy-quark limit [5], it is possible to use heavy-quark ef-

[1] Also, the lowest chosen values of m_Q are around 1 GeV, which may be too small to be considered "heavy."

fective theory (HQET) or NRQCD to describe short-distance effects, including the lattice artifacts of the heavy quark [4]. This last remedy is explained in detail in Sec. II C, where we show also how all three strategies are connected.

B. HQET description of QCD

The breakdown of the standard Symanzik description of cutoff effects for Wilson fermions arises because the kinematics of heavy hadron decays single out a vector, namely, the heavy hadron velocity. But, since the heavy-quark mass is also much larger than the spatial momenta of the problem, the dynamics simplify. In continuum QCD, this has led to the development of the effective field theories HQET [26,27,34–36] and NRQCD [3,25]. These two effective theories are useful for generating an expansion in $\boldsymbol{p}/m_Q$. They share a common effective Lagrangian, but the power in $\boldsymbol{p}/m_Q$ assigned to any given operator is not necessarily the same. In HQET the power can be deduced immediately from the dimension, whereas in NRQCD it is deduced by counting powers of the relative velocity of the $\overline{Q}Q$ system. The discussion in this paper will follow the counting of HQET, but the logic could be repeated with the counting of NRQCD.

Our aim is to show, for the case of heavy-light currents, how to use HQET to extend the standard Symanzik program into the region where $m_Q a$ is no longer small. This program was started in Ref. [4], building on Ref. [5]. The formalism holds for all $m_Q a$, but, like the usual HQET, it requires

$$m_Q \gg \boldsymbol{p}, \Lambda_{\mathrm{QCD}}. \tag{2.16}$$

First, in this subsection, we recall the HQET description of continuum QCD, paralleling the discussion in Sec. II A. Then, in Sec. II C, we explain what changes are needed to describe the cutoff effects of lattice NRQCD and of lattice gauge theory with Wilson fermions.

The HQET conventions are the same as those given Sec. III of Ref. [4]. The velocity needed to construct HQET is v. The fourth Euclidean component $v_4 = iv^0$, so in the rest frame $v=(i,\mathbf{0})$. The metric is taken to be diag$(\pm 1,1,1,1)$, with the upper (lower) sign for Euclidean (Minkowski) spacetime. In either case, $v^2=-1$. The heavy quark field is called h_v, and it satisfies the constraint $\frac{1}{2}(1-i\not{v})h_v = h_v$, or

$$\not{h}_v = i h_v, \quad \overline{h_v}\not{v} = i\overline{h_v}. \tag{2.17}$$

Physically Eq. (2.17) means that h_v describes only quarks, but not anti-quarks. The tensor $\eta_\nu^\mu = \delta_\nu^\mu + v^\mu v_\nu$ projects onto components orthogonal to v. For a vector p, the component orthogonal to v is $p_\perp^\mu = \eta_\nu^\mu p^\nu = p^\mu + v^\mu (v\cdot p)$; in the rest frame, these are the spatial components.

HQET describes the dynamics of heavy-light bound states with an effective Lagrangian built from h_v. So, for these states, one can say

$$\mathcal{L}_{\mathrm{QCD}} \doteq \mathcal{L}_{\mathrm{HQET}}, \tag{2.18}$$

where

$$\mathcal{L}_{\mathrm{HQET}} = \mathcal{L}^{(0)} + \mathcal{L}^{(1)} + \mathcal{L}^{(2)} + \cdots. \tag{2.19}$$

For HQET $\mathcal{L}^{(s)}$ contains terms of dimension $4+s$. Note that the ultraviolet regulator and renormalization scheme of the two sides of Eq. (2.18) need not be the same, although dimensional regularization and the modified minimal subtraction ($\overline{\mathrm{MS}}$) scheme are usually used for both.

For this paper it is enough to consider the first two terms, $\mathcal{L}^{(0)}$ and $\mathcal{L}^{(1)}$. The leading, dimension-four term is

$$\mathcal{L}^{(0)} = \overline{h_v}(iv\cdot D - m)h_v. \tag{2.20}$$

The choice of v is somewhat arbitrary. If v is close to the heavy quark's velocity,[2] then $\mathcal{L}^{(0)}$ is a good starting point for the heavy-quark expansion, which treats the higher-dimension operators as small. The most practical choice is the velocity of the hadron containing the heavy quark.

The mass term in $\mathcal{L}^{(0)}$ is often omitted. By heavy-quark symmetry, it has an effect neither on bound-state wave functions nor, consequently, on matrix elements. It does affect the mass spectrum, but only additively. Including the mass obscures the heavy-quark flavor symmetry, but only slightly [4]. When the mass term is included, higher-dimension operators are constructed with $\mathcal{D}^\mu = D^\mu - imv^\mu$ [32]. To describe on-shell matrix elements one may omit operators that vanish by the equation of motion, $-iv\cdot\mathcal{D}h_v = 0$, derived from Eq. (2.20). In practice, therefore, higher-dimension operators are constructed from $\mathcal{D}_\perp^\mu = D_\perp^\mu$ and $[\mathcal{D}^\mu,\mathcal{D}^\nu] = [D^\mu,D^\nu] = F^{\mu\nu}$.

The dimension-five interactions are

$$\mathcal{L}^{(1)} = \mathcal{C}_2\mathcal{O}_2 + \mathcal{C}_\mathcal{B}\mathcal{O}_\mathcal{B}, \tag{2.21}$$

where $\mathcal{C}_2$ and $\mathcal{C}_\mathcal{B}$ are short-distance coefficients, and

$$\mathcal{O}_2 = \overline{h_v} D_\perp^2 h_v, \tag{2.22}$$

$$\mathcal{O}_\mathcal{B} = \overline{h_v} s_{\alpha\beta} B^{\alpha\beta} h_v, \tag{2.23}$$

with $s_{\alpha\beta} = -i\sigma_{\alpha\beta}/2$ and $B^{\alpha\beta} = \eta_\mu^\alpha \eta_\nu^\beta F^{\mu\nu}$.

In Eq. (2.20) one should think of the quark mass m as a short-distance coefficient. By reparametrization invariance [37], the same mass appears in the denominator of the kinetic energy $\mathcal{C}_2\mathcal{O}_2$, namely,

$$\mathcal{C}_2 = \frac{1}{2m}. \tag{2.24}$$

If operator insertions in HQET are renormalized with a minimal subtraction in dimensional regularization, then m is the (perturbative) pole mass. With other ultraviolet regulators, the operator and the mass m could become μ-dependent. Even in mass-independent schemes, the chromomagnetic operator $\mathcal{O}_\mathcal{B}$ depends on the renormalization point μ of the HQET, and that dependence is canceled by

[2] In NRQCD applications the relative velocity between the heavy quark and heavy anti-quark should not be confused with the velocity v introduced here.

$$C_{\mathcal{B}}(\mu)=\frac{z_{\mathcal{B}}(\mu)}{2m}, \tag{2.25}$$

with $2m$ appearing so that $z_{\mathcal{B}}$ is unity at the tree level.

The description of electroweak flavor-changing operators proceeds along the same lines. The flavor-changing vector current for a $b\to q$ transition, defined to be $\mathcal{V}^\mu=\overline{q}i\gamma^\mu b$ as in Eq. (2.7), is described in HQET by

$$\mathcal{V}^\mu \doteq C_{V_\parallel} v^\mu \overline{q} h_v + C_{V_\perp} \overline{q} i\gamma_\perp^\mu h_v - \sum_{i=1}^{6} B_{Vi} \mathcal{Q}_{Vi}^\mu + \cdots, \tag{2.26}$$

where h_v is the HQET field, which satisfies Eq. (2.19) and whose dynamics are given by $\mathcal{L}_{\rm HQET}$. The dimension-four operators are

$$\mathcal{Q}_{V1}^\mu = -v^\mu \overline{q} i\not{D}_\perp h_v, \tag{2.27}$$

$$\mathcal{Q}_{V2}^\mu = \overline{q} i\gamma_\perp^\mu i\not{D}_\perp h_v, \tag{2.28}$$

$$\mathcal{Q}_{V3}^\mu = \overline{q} i D_\perp^\mu h_v, \tag{2.29}$$

$$\mathcal{Q}_{V4}^\mu = +v^\mu \overline{q} i\overleftarrow{\not{D}}_\perp h_v, \tag{2.30}$$

$$\mathcal{Q}_{V5}^\mu = \overline{q} i\overleftarrow{\not{D}}_\perp i\gamma_\perp^\mu h_v, \tag{2.31}$$

$$\mathcal{Q}_{V6}^\mu = \overline{q} i\overleftarrow{D}_\perp^\mu h_v. \tag{2.32}$$

Further dimension-four operators are again omitted, because they are linear combinations of those listed and others that vanish by the equations of motion. For example, $\overline{q}(iv\cdot\overleftarrow{D})v^\mu h_v = \overline{q}(i\overleftarrow{\not{D}}_\perp - i\overleftarrow{\not{D}})v^\mu h_v = \mathcal{Q}_{V4}^\mu - m_q v^\mu \overline{q} h_v$, where the Dirac equation is used for the last step.

The axial vector current $\mathcal{A}^\mu=\overline{q}i\gamma^\mu\gamma_5 b$ has a completely analogous description,

$$\mathcal{A}^\mu \doteq C_{A_\perp} \overline{q} i\gamma_\perp^\mu \gamma_5 h_v - C_{A_\parallel} v^\mu \overline{q}\gamma_5 h_v - \sum_{i=1}^{6} B_{Ai} \mathcal{Q}_{Ai}^\mu + \cdots, \tag{2.33}$$

where each operator $\mathcal{Q}_{Ai}^\mu$ is obtained from $\mathcal{Q}_{Vi}^\mu$ by replacing $\overline{q}$ with $-\overline{q}\gamma_5$.

The short-distance coefficients of HQET depend on the heavy-quark mass m, as well as μ/m and m_q/m, where μ is the the renormalization scale and m_q is the light quark mass. They are not explicitly needed in this paper, but it may be instructive to give the coefficients of the dimension-three terms through one-loop order, with $m_q=0$ $(J=V,A)$ [27]:

$$C_{J_\parallel} = 1 + \frac{g^2 C_F}{16\pi^2}[\gamma_h \ln(m^2/\mu^2) - 2], \tag{2.34}$$

$$C_{J_\perp} = 1 + \frac{g^2 C_F}{16\pi^2}[\gamma_h \ln(m^2/\mu^2) - 4], \tag{2.35}$$

where the anomalous dimension $\gamma_h=3/2$. The μ-independent part of $C_{A_\parallel}$ and $C_{A_\perp}$ given here assumes that the axial current is renormalized in a chirally symmetric way [38]. The coefficients of the dimension-four currents are

$$B_{Ji}^{[0]} = \frac{1}{2m}, \quad i\leqslant 2, \tag{2.36}$$

$$B_{Ji}^{[0]} = 0, \quad i\geqslant 3, \tag{2.37}$$

at the tree level, but all B_{Ji} become non-trivial when radiative corrections are included.

C. HQET description of lattice gauge theory

HQET provides a systematic way to separate the short distance $1/m$ from the scale $\Lambda_{\rm QCD}$ in heavy-light matrix elements, as long as the condition (2.16) holds. The formalism can also be applied to lattice gauge theory, again as long as condition (2.16) holds (and $\boldsymbol{p}a\ll 1$). When lattice NRQCD is used for heavy-light systems, this is because $\mathcal{L}_{\rm HQET}$ is just the Symanzik LE$\mathcal{L}$ for lattice NRQCD. When Wilson fermions are used for heavy quarks, one may also apply HQET, because they have the same particle content and heavy-quark symmetries [4]. In both cases bilinears of lattice fermions fields are introduced to approximate the continuum QCD currents. One field corresponds to the light quark, and the other to the heavy quark. An explicit construction, through order $1/m$, is in Ref. [29] for lattice NRQCD, and a similar construction for Wilson fermions is in Sec. III. Lattice artifacts stemming from the light quark can be described as in Sec. II A, but lattice artifacts of the heavy quark should be lumped into the HQET short-distance coefficients. Some of the operators needed to describe heavy-quark discretization effects do not appear in the usual HQET description of continuum QCD. For example, the dimension-seven operator $\Sigma_i \overline{h}_v D_i^4 h_v$ (written here in the rest frame) appears in $\mathcal{L}^{(3)}$ to describe the breaking of rotational invariance on the lattice. Similarly, at and beyond dimension five there are HQET current operators to describe violations of rotational symmetry in the lattice currents. Because of the high dimension, these effects lie beyond the scope of this paper, which concentrates on operators of leading and next-to-leading dimension.

In this way, the preceding description of continuum QCD can be repeated for lattice gauge theory with the same logic and structure. Instead of Eq. (2.1), one introduces a relation like Eq. (2.18),

$$\mathcal{L}_{\rm lat} \doteq \mathcal{L}_{\rm HQET}, \tag{2.38}$$

where $\mathcal{L}_{\rm lat}$ is a lattice Lagrangian for NRQCD or Wilson quarks, and $\mathcal{L}_{\rm HQET}$ is an HQET Lagrangian with the same operators as in Eqs. (2.20) and (2.21), but modified coefficients. In the dimension-four HQET Lagrangian $\mathcal{L}^{(0)}$, one must now replace m with the heavy quark rest mass m_1. The

other coefficients will be denoted $C_i^{\rm lat}$. In particular, in $\mathcal{L}^{(1)}$ the coefficient of the kinetic energy becomes

$$C_2^{\rm lat}=\frac{1}{2m_2}. \tag{2.39}$$

If operator insertions of $\mathcal{O}_2$ continue to be defined by dimensional regularization with minimal subtraction, then both the rest mass m_1 and the kinetic mass m_2 generalize the perturbative pole mass. Like the usual pole mass, they are properties of the pole in the perturbative quark propagator [31], and they are infrared finite and gauge independent [39]. The lattice breaks Lorentz (or Euclidean) invariance, so reparametrization invariance no longer requires m_2 to be the same as m_1.

Similarly, a heavy-light lattice (axial) vector current $V_{\rm lat}^\mu$ ($A_{\rm lat}^\mu$) can be described by

$$V_{\rm lat}^\mu \doteq C_{V_\parallel}^{\rm lat} v^\mu \overline{q} h_v + C_{V_\perp}^{\rm lat} \overline{q} i\gamma_\perp^\mu h_v - \sum_{i=1}^{6} B_{Vi}^{\rm lat} \mathcal{Q}_{Vi}^\mu + \cdots, \tag{2.40}$$

$$A_{\rm lat}^\mu \doteq C_{A_\perp}^{\rm lat} \overline{q} i\gamma_\perp^\mu \gamma_5 h_v - C_{A_\parallel}^{\rm lat} v^\mu \overline{q}\gamma_5 h_v - \sum_{i=1}^{6} B_{Ai}^{\rm lat} \mathcal{Q}_{Ai}^\mu + \cdots, \tag{2.41}$$

but there are two important changes from Eq. (2.26). First, the light quarks (and gluons) are now also on the lattice, so they are described by their usual Symanzik LE$\mathcal{L}$s. Second, the short-distance coefficients of HQET are modified, because the lattice modifies the dynamics at short distances. The coefficients $C_{J_\parallel}^{\rm lat}$, $C_{J_\perp}^{\rm lat}$, and $B_{Ji}^{\rm lat}$ now depend on the lattice spacing a, i.e., on ma, in addition to m, μ/m, and m_q/m. A heavy-light lattice axial vector current has an analogous description.

On the other hand, in Eqs. (2.26) and (2.40) the HQET operators are the same. As a rule, the ultraviolet regulator of an effective theory does not have to be the same as that of the underlying theory. (The standard Symanzik program works this way.) Thus, when describing lattice gauge theory one is free to regulate HQET just as one would when describing continuum QCD. Moreover, since Eqs. (2.27)–(2.32) give a complete set of dimension-four HQET currents, the coefficients $C_{J_\parallel,J_\perp}^{\rm lat}$ and $B_{Ji}^{\rm lat}$ contain short-distance effects from both the light and the heavy sectors.

By comparing the HQET descriptions of lattice and continuum QCD, one can see how lattice matrix elements differ from their continuum counterparts. The continuum matrix element of $v\cdot\mathcal{V}$, for example, is

$$\begin{aligned}\langle L|v\cdot\mathcal{V}|B\rangle =& -C_{V_\parallel}\langle L|\overline{q}h_v|B_v^{(0)}\rangle - B_{V1}\langle L|v\cdot\mathcal{Q}_{V1}|B_v^{(0)}\rangle - B_{V4}\langle L|v\cdot\mathcal{Q}_{V4}|B_v^{(0)}\rangle - \mathcal{C}_2 C_{V_\parallel}\int d^4x\langle L|T\,\mathcal{O}_2(x)\overline{q}h_v|B_v^{(0)}\rangle^\star \\ & - \mathcal{C}_{\mathcal{B}} C_{V_\parallel}\int d^4x\langle L|T\,\mathcal{O}_{\mathcal{B}}(x)\overline{q}h_v|B_v^{(0)}\rangle^\star + O(\Lambda^2/m^2),\end{aligned} \tag{2.42}$$

where L is any light hadronic state, including the vacuum. (The starred T product is defined in Ref. [4]; this detail is unimportant here.) On the left-hand side B denotes a b-flavored hadron, and on the right-hand side $B_v^{(0)}$ denotes the corresponding eigenstate of the leading effective Lagrangian $\mathcal{L}^{(0)}$. Similarly, the lattice matrix element is [4]

$$\begin{aligned}\langle L|v\cdot V_{\rm lat}|B\rangle =& -C_{V_\parallel}^{\rm lat}\langle L|\overline{q}h_v|B_v^{(0)}\rangle - B_{V1}^{\rm lat}\langle L|v\cdot\mathcal{Q}_{V1}|B_v^{(0)}\rangle - B_{V4}^{\rm lat}\langle L|v\cdot\mathcal{Q}_{V4}|B_v^{(0)}\rangle - \mathcal{C}_2^{\rm lat} C_{V_\parallel}^{\rm lat}\int d^4x\langle L|T\mathcal{O}_2(x)\overline{q}h_v|B_v^{(0)}\rangle^\star \\ & - \mathcal{C}_{\mathcal{B}}^{\rm lat} C_{V_\parallel}^{\rm lat}\int d^4x\langle L|T\mathcal{O}_{\mathcal{B}}(x)\overline{q}h_v|B_v^{(0)}\rangle^\star - K_{\sigma\cdot F} C_{V_\parallel}^{\rm lat}\int d^4x\langle L|T\,\overline{q}i\sigma F q(x)\overline{q}h_v|B_v^{(0)}\rangle^\star + O(\Lambda^2 a^2 b(ma)).\end{aligned} \tag{2.43}$$

Compared to Eq. (2.42), the short-distance coefficients are modified to depend on ma, there is an extra term from the Symanzik LE$\mathcal{L}$ of the light quark, and the next power corrections can, in general, be multiplied by a (bounded) function of ma. The matrix elements on the right-hand sides are, however, identical, because in both cases they are defined with $\mathcal{L}^{(0)}$ describing the heavy quark and $\mathcal{L}_{\rm QCD}$ describing the light quark (and gluons).

Similar equations hold for matrix elements of $\mathcal{V}_\perp$ and $V_{\perp\,\rm lat}$, and for the axial vector current. If one multiplies the equations for the lattice matrix elements with

$$Z_{J_\parallel} = \frac{C_{J_\parallel}}{C_{J_\parallel}^{\rm lat}}, \tag{2.44}$$

$$Z_{J_\perp} = \frac{C_{J_\perp}}{C_{J_\perp}^{\rm lat}}, \tag{2.45}$$

and subtracts the result from the continuum equations, one finds that the difference can be traced solely to the mismatch of the short-distance coefficients, or

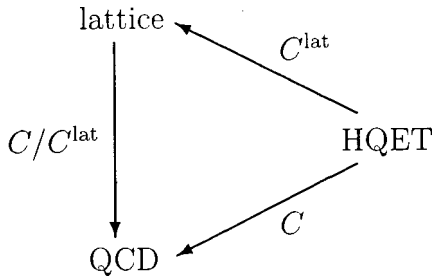

FIG. 1. Diagram illustrating how the matching factors $C^{\rm lat}$, C, and $Z=C/C^{\rm lat}$ match lattice gauge theory and QCD to HQET, and to each other.

$$\delta\mathcal{C}_i=\mathcal{C}_i^{\rm lat}-\mathcal{C}_i\,, \tag{2.46}$$

$$\delta B_{Ji}=Z_{Ji}B_{Ji}^{\rm lat}-B_{Ji}\,, \tag{2.47}$$

where the normalization factors Z_{Ji} are $Z_{J_\parallel}$ for $i=1$, 4, and $Z_{J_\perp}$ for $i=2,3,5,6$. In Eqs. (2.46) and (2.47) a picture emerges, where *heavy-quark lattice artifacts are isolated* into $\delta\mathcal{C}_i$ and δB_{Ji}. Furthermore, the analysis presented here makes no explicit reference to any method for computing the short-distance coefficients, so it applies at every order in perturbation theory (in g^2) and, presumably, at a nonperturbative level as well.

The matching factors $Z_{J_\parallel}$ and $Z_{J_\perp}$ play the following role, sketched in Fig. 1. In each case, the denominator converts a lattice-regulated scheme to a renormalized HQET scheme, and the numerator converts the latter to a renormalized (continuum) QCD scheme. As long as the same HQET scheme is used, HQET drops out of the calculation of $Z_{J_\parallel}$ and $Z_{J_\perp}$. Moreover, changes in continuum renormalization conventions modify only the numerator, and changes in the lattice action or currents modify only the denominator. In a similar way, dependence on the HQET renormalization scheme drops out when computing $\delta\mathcal{C}_i$ and δB_{Ji}.

One can derive a connection between the matching coefficients of the HQET and the Symanzik descriptions when $ma\ll 1$ and $m\gg\boldsymbol{p}$, so that both formalisms apply. With the Lagrangian, one applies HQET to Eqs. (2.2)–(2.4) and identifies the short-distance coefficients with m_1, $\mathcal{C}_2^{\rm lat}$, and $\mathcal{C}_{\mathcal{B}}^{\rm lat}$. Then one finds,

$$m_{1b}=m_b+O(a^2), \tag{2.48}$$

$$m_{2b}=m_b+O(a^2), \tag{2.49}$$

$$z_{\mathcal{B}}^{\rm lat}=z_{\mathcal{B}}-4m_b aK_{\sigma\cdot F}C_{\sigma\cdot F}\,, \tag{2.50}$$

where the short-distance coefficient $C_{\sigma\cdot F}$ appears in the relation

$$\overline{b}i\sigma^{\mu\nu}F_{\mu\nu}b\doteq -2C_{\sigma\cdot F}\mathcal{O}_{\mathcal{B}}. \tag{2.51}$$

At the tree level, $C_{\sigma\cdot F}^{[0]}=1$. For the [axial] vector current, one inserts Eq. (2.26) [Eq. (2.33)] into Eq. (2.5) [Eq. (2.6)], neglects terms of order m^2a^2, and compares with Eq. (2.40) [Eq. (2.41)]. One also must match the tensor and pseudoscalar bilinears to HQET at the dimension-three level,

$$\overline{q}i\sigma^{\mu\nu}b\doteq C_{T_+}\eta_\alpha^\mu\eta_\beta^\nu\overline{q}i\sigma^{\alpha\beta}h_v-C_{T_-}\overline{q}(v^\mu i\gamma_\perp^\nu-v^\nu i\gamma_\perp^\mu)h_v\,, \tag{2.52}$$

$$\overline{q}i\gamma_5 b\doteq C_P\overline{q}i\gamma_5 h_v\,, \tag{2.53}$$

with short-distance coefficients $C_{T_\pm}$ and C_P. At the tree level, $C_{T_\pm}^{[0]}=C_P^{[0]}=1$. After carrying out these steps, one finds that

$$Z_{V_\parallel}=Z_V\,, \tag{2.54}$$

$$Z_{V_\perp}^{-1}=Z_V^{-1}+(m_q+m_b)aK_VC_{T_-}/C_{V_\perp}, \tag{2.55}$$

$$Z_{V_\parallel}B_{V1}^{\rm lat}=B_{V1}+aZ_VK_VC_{T_-}, \tag{2.56}$$

$$Z_{V_\parallel}B_{Vi}^{\rm lat}=B_{Vi}+aZ_VK_VC_{T_+},\quad i=2,6, \tag{2.57}$$

$$Z_{V_\parallel}B_{V3}^{\rm lat}=B_{V3}-aZ_VK_VC_{T_+}, \tag{2.58}$$

$$Z_{V_\parallel}B_{V4}^{\rm lat}=B_{V4}-aZ_VK_VC_{T_-}, \tag{2.59}$$

$$Z_{V_\parallel}B_{V5}^{\rm lat}=B_{V5}-aZ_VK_V(C_{T_+}-C_{T_-}) \tag{2.60}$$

from matching the vector current, and

$$Z_{A_\perp}=Z_A\,, \tag{2.61}$$

$$Z_{A_\parallel}^{-1}=Z_A^{-1}+(m_q+m_b)aK_AC_P/C_{A_\parallel}, \tag{2.62}$$

$$Z_{A_\perp}B_{Ai}^{\rm lat}=B_{Ai}+O(a^2),\quad i=1,2,5, \tag{2.63}$$

$$Z_{A_\perp}B_{Ai}^{\rm lat}=B_{Ai}+aZ_AK_AC_P\,,\quad i=3,6, \tag{2.64}$$

$$Z_{A_\perp}B_{A4}^{\rm lat}=B_{A4}-aZ_AK_AC_P, \tag{2.65}$$

from matching the axial vector current. Of course, these relations hold only when describing the same lattice currents $V_{\rm lat}^\mu$ and $A_{\rm lat}^\mu$, and then only to order a^2. Considering similar relations for the whole tower of higher-dimension operators, one sees

$$\lim_{a\to 0}\mathcal{C}_{\mathcal{O}}^{\rm lat}=\mathcal{C}_{\mathcal{O}}, \tag{2.66}$$

$$\lim_{a\to 0}Z_{Ji}B_{Ji}^{\rm lat}=B_{Ji}\,. \tag{2.67}$$

Equations (2.55)–(2.60) and (2.62)–(2.65) illustrate for the next-to-leading dimension operators how the limit is accelerated for standard $O(a)$ improvement, with $K_{\sigma\cdot F}$, K_V, and K_A themselves of order a.

Equations (2.54)–(2.65) show that HQET matching connects smoothly to Symanzik matching in the limit where both apply. HQET matching is, therefore, a natural and attractive extension into the more practical region where ma is

not very small. Continuum QCD still can be approximated well, but now order by order in the heavy-quark expansion.

The remainder of this paper pursues this program in perturbation theory. One-loop corrections to the rest mass m_1 and the kinetic mass m_2 have been considered already in Ref. [31]. The one-loop correction to $\mathcal{C}_\mathcal{B}$ would require a generalization of the calculation of $K_{\sigma\cdot F}$ [33] to incorporate the full mass dependence of the quark-gluon vertex. In this paper we focus on heavy-light currents. We construct lattice currents suitable for matching through order $1/m_Q$ in the heavy quark expansion. We then calculate the matching factors $Z_{J_\parallel}$ and $Z_{J_\perp}$ at the one-loop level, which are needed to fix the overall normalization of the heavy-light currents. Currents suitable for heavy-to-heavy transitions $b\to c$ are considered in a companion paper [6].

III. LATTICE ACTION AND CURRENTS

In this section our aim is to define heavy-light currents with Wilson fermions that are suited to the HQET matching formalism. Because Wilson fermions have the right particle content and obey the heavy-quark symmetries, the descriptive part of the formalism applies in any case. To use HQET to match lattice gauge theory to continuum QCD, however, we would like to ensure that $\delta\mathcal{C}_i$ and δB_{Ji} [cf. Eqs. (2.46) and (2.47)] remain bounded in the infinite-mass limit. Good behavior is attained by mimicking the structure of Eqs. (2.27)–(2.32), so that improvement terms are guaranteed to remain small. Then we would like to adjust free parameters in the currents so that $\delta\mathcal{C}_i$ and δB_{Ji} (approximately) vanish. We show how to do so in perturbation theory, obtaining $B_{Ji}^{\rm lat}$ at the tree level and, in Sec. IV, the matching factors $Z_{J_\parallel}$ and $Z_{J_\perp}$ at the one-loop level.

A suitable lattice Lagrangian was introduced in Ref. [5]. It is convenient to write the lattice Lagrangian $\mathcal{L}_{\rm lat}=\mathcal{L}_0+\mathcal{L}_B+\mathcal{L}_E$. The first term is

$$\begin{aligned}\mathcal{L}_0=&-(m_0+m_{0\rm cr})\overline{\psi}(x)\psi(x)-\tfrac{1}{2}\overline{\psi}(x)\\&\times[(1+\gamma_4)D_{4\ \rm lat}^{-}-(1-\gamma_4)D_{4\ \rm lat}^{+}]\psi(x)\\&-\zeta\overline{\psi}(x)\boldsymbol{\gamma}\cdot\boldsymbol{D}_{\rm lat}\psi(x)+\tfrac{1}{2}r_s\zeta a\overline{\psi}(x)\triangle_{\rm lat}^{(3)}\psi(x).\end{aligned}\tag{3.1}$$

The mass counterterm $m_{0\rm cr}$ is included here so that, by definition, $m_0=0$ for massless quarks. The covariant difference operators $D_{4\ \rm lat}^{\pm}$, $\boldsymbol{D}_{\rm lat}$, and $\triangle_{\rm lat}^{(3)}$, are defined in Ref. [5]. They carry the label "lat" to distinguish them from the continuum covariant derivatives in Secs. II A and II B. The symbol ψ is reserved in this paper for lattice fermion fields. The temporal kinetic term is conventionally normalized, but the spatial kinetic term is multiplied with the coupling ζ. The coupling r_s is, in the technical sense, redundant [5], but is included to solve the doubling problem [17].

For $\mathcal{L}_0$ the tree-level relations between its couplings and the coefficients in the $\mathcal{L}_{\rm HQET}$ are well known. By matching the kinetic energy, one finds (for $\boldsymbol{v}=\boldsymbol{0}$)

$$\mathcal{C}_2^{\rm lat[0]}=\frac{1}{2m_2^{[0]}a}=\frac{\zeta^2}{m_0a(2+m_0a)}+\frac{r_s\zeta}{2(1+m_0a)}.\tag{3.2}$$

At higher orders in perturbation theory, $\mathcal{C}_2$ remains (for $\boldsymbol{v}=\boldsymbol{0}$) the kinetic mass of the quark, which is expressed in terms of the self-energy in Ref. [31].

$\mathcal{L}_0$ has cutoff artifacts, which are described by dimension-five and -higher operators in $\mathcal{L}_{\rm Sym}$ (if $m_qa\ll 1$) or $\mathcal{L}_{\rm HQET}$ (if $m_Q\gg\Lambda_{\rm QCD}$). The dimension-five effect can be reduced by adding

$$\mathcal{L}_B=\frac{i}{2}ac_B\zeta\overline{\psi}(x)\boldsymbol{\Sigma}\cdot\boldsymbol{B}_{\rm lat}(x)\psi(x),\tag{3.3}$$

$$\mathcal{L}_E=\tfrac{1}{2}ac_E\zeta\overline{\psi}(x)\boldsymbol{\alpha}\cdot\boldsymbol{E}_{\rm lat}(x)\psi(x),\tag{3.4}$$

and suitably adjusting of c_B and c_E. The lattice chromomagnetic and chromoelectric fields, $\boldsymbol{B}_{\rm lat}$ and $\boldsymbol{E}_{\rm lat}$, are those given in Ref. [5].

By matching the gluon-quark vertex, one finds

$$\mathcal{C}_\mathcal{B}^{\rm lat[0]}=\frac{1}{2m_\mathcal{B}^{[0]}a}=\frac{\zeta^2}{m_0a(2+m_0a)}+\frac{c_B\zeta}{2(1+m_0a)}.\tag{3.5}$$

Higher-order corrections to $\mathcal{C}_\mathcal{B}^{\rm lat}$ have not been obtained. By comparing Eqs. (3.2) and (3.5) one sees, however, that $c_B=r_s+O(g^2)$ is needed to adjust $\mathcal{C}_\mathcal{B}^{\rm lat}$ to its continuum counterpart $\mathcal{C}_\mathcal{B}=z_\mathcal{B}/2m_2$.

The Euclidean action is $S=-a^4\Sigma_x\mathcal{L}(x)$. Special cases are the Wilson action [17], which sets $r_s=\zeta=1$, $c_B=c_E=0$; and the Sheikholeslami-Wohlert action [16], which sets $r_s=\zeta=1$, $c_B=c_E\equiv c_{\rm SW}$. But to remove lattice artifacts for arbitrary masses, the couplings r_s, ζ, c_B and c_E must be taken to depend on m_0a [5]. Our analytical results for the integrands of Feynman diagrams, given in Appendix B, are for arbitrary choices of these couplings. Indeed, our expressions allow the heavy and light quarks to have different values of all couplings.

Heavy-light currents are defined in an essentially similar way. For convenience, first define a "rotated" field [18,5]

$$\Psi_q=[1+ad_1\boldsymbol{\gamma}\cdot\boldsymbol{D}_{\rm lat}]\psi_q,\tag{3.6}$$

where ψ_q is the field in $\mathcal{L}_0$ of flavor q, and $\boldsymbol{D}_{\rm lat}$ is again the symmetric covariant difference operator. Simple bilinears with the right quantum numbers are

$$V_0^\mu=\overline{\Psi}_q i\gamma^\mu\Psi_b,\tag{3.7}$$

$$A_0^\mu=\overline{\Psi}_q i\gamma^\mu\gamma_5\Psi_b.\tag{3.8}$$

The subscript "0" implies that, as with $\mathcal{L}_0$, some improvement is desired. To ensure a good large-ma limit, one should pattern the improved current after the right-hand side of Eq. (2.40). Thus, we take

$$V_{\rm lat}^\mu=V_0^\mu-\sum_{i=1}^{6}b_{Vi}Q_{Vi}^\mu,\tag{3.9}$$

$$A^\mu_{\rm lat} = A^\mu_0 - \sum_{i=1}^{6} b_{Ai} Q^\mu_{Ai}, \tag{3.10}$$

where the b_{Ji} are adjustable, and the dimension-four lattice operators are

$$Q^\mu_{V1} = -v^\mu \overline{\psi}_q i \not{v} \not{D}_{\perp\,\rm lat} \psi_b, \tag{3.11}$$

$$Q^\mu_{V2} = \overline{\psi}_q i \gamma^\mu_\perp \not{D}_{\perp\,\rm lat} \psi_b, \tag{3.12}$$

$$Q^\mu_{V3} = \overline{\psi}_q i D^\mu_{\perp\,\rm lat} \psi_b, \tag{3.13}$$

$$Q^\mu_{V4} = -v^\mu \overline{\psi}_q \overleftarrow{\not{D}}_{\perp\,\rm lat} i \not{v} \psi_b, \tag{3.14}$$

$$Q^\mu_{V5} = \overline{\psi}_q \overleftarrow{\not{D}}_{\perp\,\rm lat} i \gamma^\mu_\perp \psi_b, \tag{3.15}$$

$$Q^\mu_{V6} = \overline{\psi}_q i \overleftarrow{D}^\mu_{\perp\,\rm lat} \psi_b, \tag{3.16}$$

and each lattice operator Q^μ_{Ai} is obtained from Q^μ_{Vi} by replacing $\overline{\psi}_q$ with $-\overline{\psi}_q \gamma_5$. Lattice quark fields do not satisfy Eq. (2.17), so $\not{v}$ appears explicitly. In practice, one uses the rest frame here, $v=(i,\mathbf{0})$, as in Eq. (3.6). An analogous construction for lattice NRQCD has been given by Morningstar and Shigemitsu [29].

It is worthwhile to emphasize the difference between Eqs. (2.40) and (3.9). Equation (2.40) is a general HQET description of any heavy-light lattice current. Equation (3.9) is a definition of a specific lattice current, namely the one used in this paper (and in calculations of f_B and other hadronic matrix elements). In the same vein, the $\mathcal{Q}_{Ji}$ in Eqs. (2.27)–(2.32) are HQET operators, whereas the Q_{Ji} in Eqs. (3.11)–(3.16) are lattice operators. Finally, the coefficients $B^{\rm lat}_{Ji}$ are the output of a matching calculation: they depend on the b_{Ji}, which must be adjusted to make δB_{Ji} vanish.

To illustrate, let us consider the calculation of the coefficients $B^{\rm lat}_{Ji}$ at the tree level. One computes on-shell matrix elements such as $\langle q|J_{\rm lat}|b\rangle$ and $\langle 0|J_{\rm lat}|\overline{q}b\rangle$ in lattice gauge theory and compares them to the corresponding matrix elements in HQET. Then one finds

$$C^{{\rm lat}[0]}_{J_\parallel} = C^{{\rm lat}\,[0]}_{J_\perp} = e^{-(m^{[0]}_{1q}+m^{[0]}_{1b})a/2}, \tag{3.17}$$

$$B^{{\rm lat}[0]}_{Ji} = e^{-(m^{[0]}_{1q}+m^{[0]}_{1b})a/2}\left(\frac{1}{2m^{[0]}_3} + b^{[0]}_{Ji}\right), \qquad i\leqslant 2 \tag{3.18}$$

$$B^{{\rm lat}[0]}_{Ji} = e^{-(m^{[0]}_{1q}+m^{[0]}_{1b})a/2} b^{[0]}_{Ji}, \qquad i\geqslant 3 \tag{3.19}$$

where

$$m^{[0]}_1 a = \ln(1+m_0 a) \tag{3.20}$$

and, for our lattice Lagrangian and currents,

$$\frac{1}{2m^{[0]}_3 a} = \frac{\zeta(1+m_0 a)}{m_0 a(2+m_0 a)} - d_1. \tag{3.21}$$

Since (continuum QCD's) $C^{[0]}_J = 1$ there already is a nontrivial matching factor at the tree level relating the lattice and continuum currents, $Z^{[0]}_{J_\parallel} = Z^{[0]}_{J_\perp} = e^{(m_{1q}+m_{1b})a/2}$.

After comparing Eqs. (3.18)–(3.19) with Eqs. (2.36)–(2.37), one sees that one can take $b^{[0]}_{Ji}=0$ for all six operators, if d_1 is adjusted correctly. At the tree level, the way to adjust d_1 is to set $m^{[0]}_3$ equal to the (tree-level) heavy-quark mass. In the effective Lagrangian there are two quark masses, the rest mass m_1 and the kinetic mass m_2. The former has no effect on matrix elements (and a trivial, additive effect on the mass spectrum). As discussed above, heavy-quark cutoff effects in matrix elements are reduced if $\mathcal{C}^{\rm lat}_2 = \mathcal{C}_2$, which means one should identify the continuum quark mass with the kinetic mass. Thus, one should set $m^{[0]}_3 = m^{[0]}_2$, which is obtained if one adjusts

$$d_1 = \frac{\zeta(1+m_0 a-\zeta)}{m_0 a(2+m_0 a)} - \frac{r_s \zeta}{2(1+m_0 a)}. \tag{3.22}$$

The same rotation also improves heavy-heavy currents at the tree level.

Beyond the tree level, it is convenient to define d_1 for the spatial component of the degenerate-mass, to the heavy-heavy current [6]. Then the corrections to the heavy-heavy current analogous to Q_{V2} and Q_{V5} would be superfluous, but for unequal masses they are still required.

For equal mass currents it is possible to compute $Z_{V_\parallel}$ nonperturbatively for all masses m_b. One may therefore prefer to write [13–15]

$$Z_{J^{ub}_{\parallel,\perp}} = \sqrt{Z_{V^{uu}_\parallel} Z_{V^{bb}_\parallel}}\, \rho_{J^{ub}_{\parallel,\perp}} \tag{3.23}$$

and compute only the factor $\rho_{J^{ub}_{\parallel,\perp}}$ in perturbation theory. To calculate the pre-factor $Z_{V^{bb}_\parallel}$ appearing in Eq. (3.23), one must have a massive quark in the final state. The definition of the heavy-heavy matching factor is given in our companion paper [6], along with a calculation of its one-loop level contribution. We give the results for heavy-light $\rho_{J_{\parallel,\perp}}$ in Sec. IV.

For a light quark, with $m_q a \ll 1$, the right hand side of Eq. (3.22) vanishes linearly in $m_0 a$. Therefore, $1-m_{3q}/m_{2q}$ is $O(m^2_q a^2)$, and the distinction between m_{3q} and m_{2q} is negligible. For this reason, and to simplify calculation, we set $m_q=0$. Then Eq. (3.22) implies $d_1=0$ for the light quark.

IV. ONE-LOOP RESULTS

In this section we present results for the matching factors at the one-loop level in perturbation theory. The one-loop contributions are known for the Wilson [11] and Sheikholeslami-Wohlert (SW) actions [12]. Both these works omit the rotation term in the current [18,5], which is needed to obtain $1/m_3$ correctly. In this section we complete the work started in Ref. [12] and report results with the clover term and with the rotation. For comparison we also present our results without the rotation, both with and without the clover term.

The computer code for generating these results is freely available [30].

The matching factors Z_J ($J=V_\parallel$, $V_\perp$, $A_\parallel$, and $A_\perp$) are simply the ratios of the lattice and continuum radiative corrections:

$$Z_J=\frac{[Z_{2h}^{1/2}\Lambda_J Z_{2l}^{1/2}]^{\rm cont}}{[Z_{2h}^{1/2}\Lambda_J Z_{2l}^{1/2}]^{\rm lat}}, \tag{4.1}$$

where Z_{2h} and Z_{2l} are wave-function renormalization factors of the heavy and light quarks, and the vertex function Λ_J is the sum of one-particle irreducible three-point diagrams, in which one point comes from the current J and the other two from the external quark states.

The expression relating Z_2 to the lattice self energy, for all masses and gauge couplings, can be found in Ref. [31]. Its dominant mass dependence is

$$Z_2\propto e^{-m_1 a}, \tag{4.2}$$

where m_1 is the all-orders rest mass (of the heavy quark). This mass dependence is not present in the vertex function or the continuum part of Eq. (4.1). Consequently, we write

$$e^{-m_1^{[0]}a/2}Z_{J_\Gamma}=1+\sum_{l=1}^{\infty} g_0^{2l}Z_{J_\Gamma}^{[l]}, \tag{4.3}$$

so that the $Z_{J_\Gamma}^{[l]}$ are only mildly mass dependent. (A slightly different convention was used in presenting results for Z_2 in Ref. [31].) By construction, this mass dependence in ρ_{J_Γ} cancels out in a gauge-invariant, all orders way. So, we write

$$\rho_{J_\Gamma}=1+\sum_{l=1}^{\infty} g_0^{2l}\rho_{J_\Gamma}^{[l]}. \tag{4.4}$$

This rest of this section is split into two subsections. In the first, we present our results for the full mass dependence of $Z_{J_\Gamma}^{[1]}$ and $\rho_{J_\Gamma}^{[1]}$. In the second, we discuss the related calculation of the Brodsky-Lepage-Mackenzie scale q^*. In both cases, we discuss fully a range of checks on our calculations.

A. $Z_J^{[1]}$ and $\rho_J^{[1]}$

The combinations of wave-function and vertex renormalization in Z_J are gauge invariant and ultraviolet and infrared finite. For vanishing light quark mass there is a collinear divergence (which can be regulated by an infinitesimally small mass), but it is common to lattice and continuum functions. In the desired ratio (4.1), the divergence cancels, and the result is independent of the scheme for regulating the collinear singularity. For large ma a remnant of this cancellation appears. The lattice theory approaches its static limit, where its ultraviolet behavior is non-logarithmic. But the region of momentum $a^{-1}<q<m$ in the continuum diagrams generates logarithms. At the one-loop level one must find $3\ln(ma)$, with the same anomalous dimension as in Eqs. (2.34) and (2.35). At higher loops the usual polynomial in $\ln(ma)$ will arise.

We have calculated the one-loop Feynman diagrams for the action specified in Eqs. (3.1)–(3.4), with arbitrary m_0, r_s, ζ, c_B, and c_E for the incoming heavy quark, and $m_0'=0$, r_s', ζ', c_B', and c_E' for the outgoing light quark. The needed Feynman rules are in Ref. [31], apart from three new rules for the current itself, which are in Appendix A. As shown in Appendix B, we have found a simple way to incorporate the rotation into the Dirac algebra. The resulting analytical expressions are surprisingly compact, and they are given explicitly in Appendixes B and C.

We have evaluated these expressions for $r_s=\zeta=1$ and $c_E=c_B\equiv c_{\rm SW}$. Thus, the numerical results correspond to the SW action ($c_{\rm SW}=1$) and to the Wilson action ($c_{\rm SW}=0$). Figure 2 plots the full mass dependence of the matching factors for the vector current, (a) $Z_{V_\parallel}$, (b) $Z_{V_\perp}$, (c) $\rho_{V_\parallel}$, and (d) $\rho_{V_\perp}$. These numerical results are for the SW action with rotation (solid lines) and also for the SW and Wilson actions without the rotation (dotted lines). Figure 3 plots the full mass dependence of the matching factors for the axial vector current, (a) $Z_{A_\parallel}$, (b) $Z_{A_\perp}$, (c) $\rho_{A_\parallel}$, and (d) $\rho_{A_\perp}$. These and the following figures are plotted against $m_1^{[0]}a$ because this variable conveniently covers the whole mass range: for small mass $m_1\approx m_2$, and for large mass $m_1 a\approx\ln m_2 a$.

We have carried out several checks on our calculations. In each case, identical numerical results have been obtained with two or more completely independent programs. The results for $Z_{J_{\parallel,\perp}}$ agree with those previously obtained, for $c_{\rm SW}=0$ [11] and for $c_{\rm SW}=1$, $d_1=0$ [12]. We have also reproduced limiting cases, as we briefly discuss below.

For $ma=0$ our calculation reduces to the usual matching calculation for massless quarks. We find (with $C_F=4/3$)

$$Z_{V_\parallel}^{[1]}=Z_{V_\perp}^{[1]}=\begin{cases}-0.129423(6), & c_{\rm SW}=1,\\ -0.174073(7), & c_{\rm SW}=0,\end{cases} \tag{4.5}$$

$$Z_{A_\parallel}^{[1]}=Z_{A_\perp}^{[1]}=\begin{cases}-0.116450(5), & c_{\rm SW}=1,\\ -0.133365(5), & c_{\rm SW}=0,\end{cases} \tag{4.6}$$

in excellent agreement with previous work for $c_{\rm SW}=1$ [40–42] and $c_{\rm SW}=0$ [42–44]. (Reference [42] gives precise results as a polynomial in $c_{\rm SW}$.)

As the mass tends to infinity, these actions and currents all lead, up to an unphysical factor, to the same vertices and quark propagator—a Wilson line. Perturbative corrections to the vertex functions must respect this universal static limit, and, therefore, they must tend to a universal value. As $ma\to\infty$, one expects the Z factors for a massive quark to approach those for the static limit, namely

$$Z_J^{[1]}=\frac{C_F}{16\pi^2}[\,\gamma_h\ln(m_2 a)^2+z_J^{[1]}], \tag{4.7}$$

where the constant $z_J^{[1]}$ depends on the current J and on $c_{\rm SW}$ (of the light quark). Since $\ln(m_2 a)\approx m_1 a$ in this region one expects the linear behavior seen in Figs. 2 and 3. The static limit is also shown in Figs. 2 and 3 with

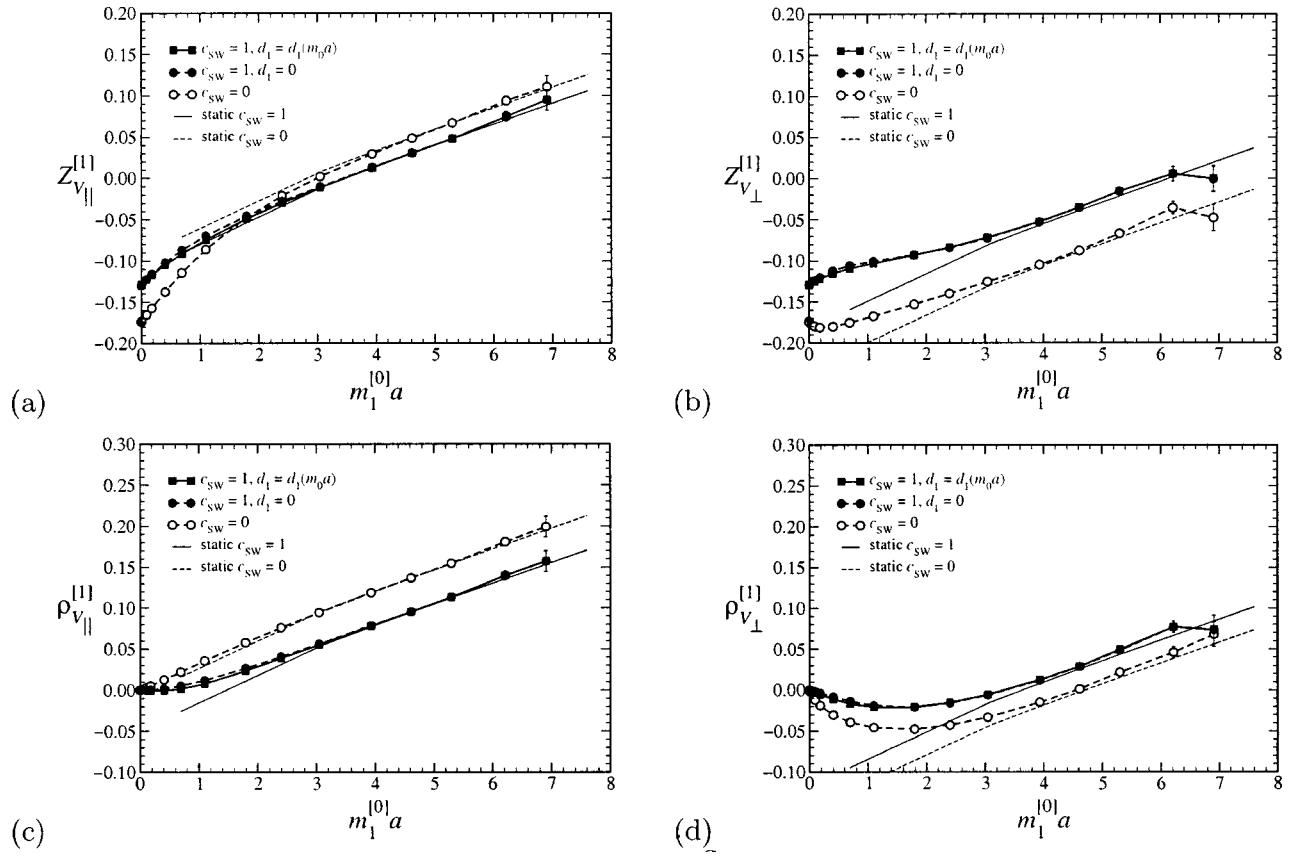

FIG. 2. Full mass dependence of the one-loop coefficients of the matching factors of the vector current (a) $Z_{V_\parallel}^{[1]}$, (b) $Z_{V_\perp}^{[1]}$, (c) $\rho_{V_\parallel}^{[1]}$, and (d) $\rho_{V_\perp}^{[1]}$. Filled (open) symbols denote the SW (Wilson) action; solid (dotted) lines connecting squares (circles) indicate the rotation is included (omitted).

$$z_{V_\parallel}^{[1]}=\begin{cases}-10.248, & c_{\rm SW}=1,\\ -7.929, & c_{\rm SW}=0,\end{cases} \tag{4.8}$$

$$z_{A_\perp}^{[1]}=\begin{cases}-8.248, & c_{\rm SW}=1,\\ -5.929, & c_{\rm SW}=0,\end{cases} \tag{4.9}$$

$$z_{V_\perp}^{[1]}=\begin{cases}-14.414, & c_{\rm SW}=1,\\ -20.379, & c_{\rm SW}=0,\end{cases} \tag{4.10}$$

$$z_{A_\parallel}^{[1]}=\begin{cases}-16.414, & c_{\rm SW}=1,\\ -22.379, & c_{\rm SW}=0.\end{cases} \tag{4.11}$$

We have obtained these constants ourselves. They agree with previous (less precise) results for $c_{\rm SW}=1$ [45] and $c_{\rm SW}=0$ [27]. As one can see from looking at Figs. 2 and 3, the static result is a good approximation for $m_1^{[0]}a>5$ or, equivalently, $m_0a\approx m_2a>150$.

Some of the points at the highest masses have large error and lie nearly one σ off the curve. The origin of this behavior is that the lattice and continuum integrals are dominated by different momenta: the continuum integral is dominated by the region $k\sim m_2\gg a^{-1}$, whereas the lattice integral is dominated by the region $k\sim a^{-1}$. This mass region is not of much practical interest, since here one has an essentially static quark.

Equations (2.54)–(2.65) allow us to check the small (heavy-quark) mass limit against the work of Sint and Weisz [46]. In our conventions the matching factors Z_V and Z_A are functions of gauge coupling and quark mass. Thus,

$$Z_V(m_qa,m_ba)=Z_V[1+\tfrac{1}{2}(m_q+m_b)ab_V], \tag{4.12}$$

$$Z_A(m_qa,m_ba)=Z_A[1+\tfrac{1}{2}(m_q+m_b)ab_A], \tag{4.13}$$

where, on the right-hand side, we adopt the notation of Refs. [9,10,46], and the Z's and b's do not depend on mass. Here only the mass dependence is displayed; all quantities depend also on the gauge coupling.

If we omit the rotation, our currents and those considered by Sint and Weisz coincide, apart from one-loop counterterms. Thus, in one-loop calculations the slopes of our mass-dependent matching factors must agree with them. Setting $m_q=0$, and using Eqs. (2.54)–(2.65),

$$\frac{\partial Z_{V_\parallel}^{[1]}}{\partial m_{1b}}=\tfrac{1}{2}b_V^{[1]}, \tag{4.14}$$

$$\frac{\partial Z_{V_\perp}^{[1]}}{\partial m_{1b}}=\tfrac{1}{2}b_V^{[1]}-K_V^{[1]}, \tag{4.15}$$

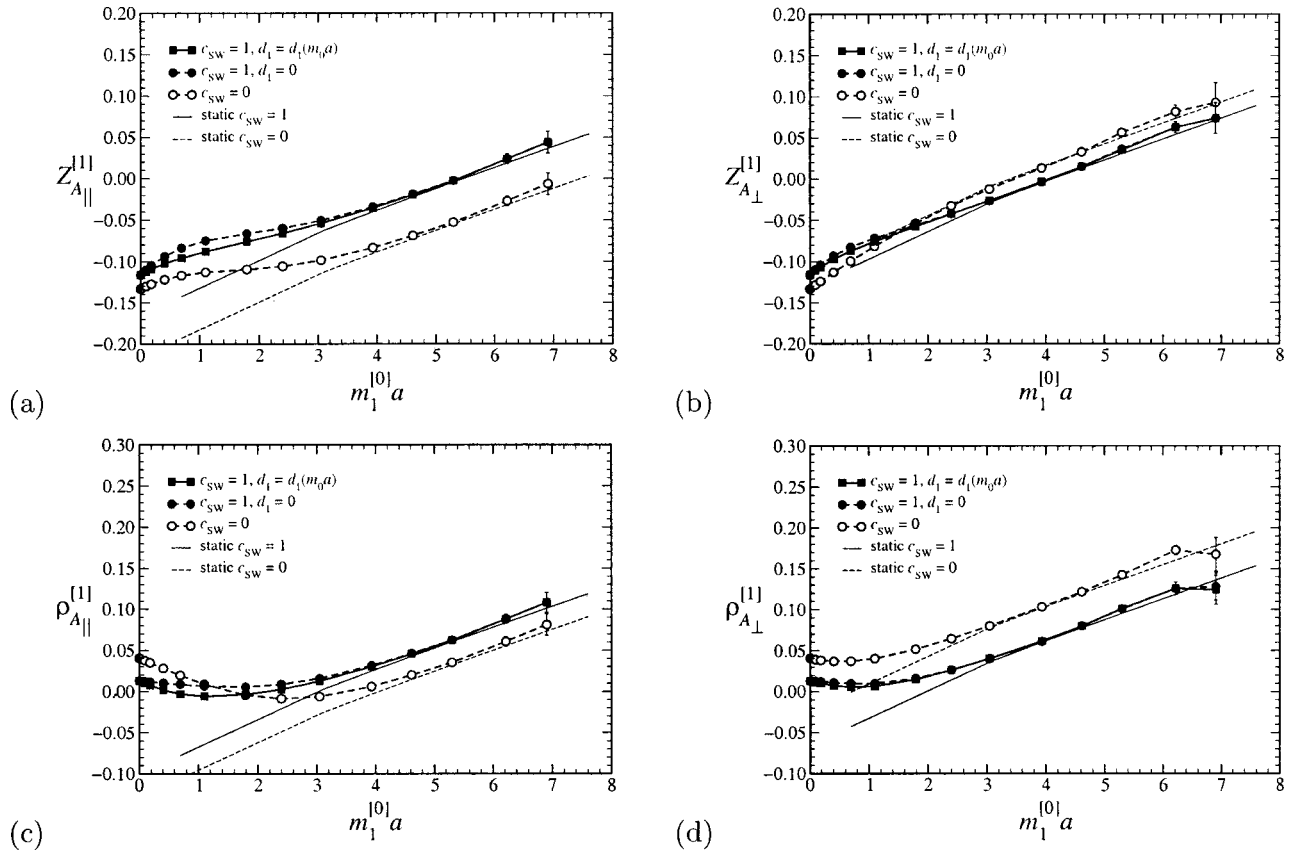

FIG. 3. Full mass dependence of the one-loop coefficients of the matching factors of the axial vector current (a) $Z_{A_\parallel}^{[1]}$, (b) $Z_{A_\perp}^{[1]}$, (c) $\rho_{A_\parallel}^{[1]}$, and (d) $\rho_{A_\perp}^{[1]}$.

$$\frac{\partial Z_{A_\parallel}^{[1]}}{\partial m_{1b}} = \tfrac{1}{2} b_A^{[1]} - K_A^{[1]}, \tag{4.16}$$

$$\frac{\partial Z_{A_\perp}^{[1]}}{\partial m_{1b}} = \tfrac{1}{2} b_A^{[1]}. \tag{4.17}$$

To extract these slopes, we form a combination of integrands with three different (small) values of $m_b a$, yielding $b_J^{[1]}$ and $K_J^{[1]}$ up to $O(m_b a)^2$. In this way we find (for $c_{\rm SW}=1$)

$$b_V^{[1]} = C_F \times 0.114929(10) = 0.153239(14) \tag{4.18}$$

vs

$$C_F \times 0.11492(4) \quad [46],$$

$$b_A^{[1]} = C_F \times 0.114142(10) = 0.152189(14) \tag{4.19}$$

vs

$$C_F \times 0.11414(4) \quad [46],$$

$$K_V^{[1]} = C_F \times 0.0122499(6) = 0.016332(7) \tag{4.20}$$

vs

$$C_F \times 0.01225(1) \quad [46],$$

$$K_A^{[1]} = C_F \times 0.0056806(11) = 0.0075741(15) \tag{4.21}$$

vs

$$C_F \times 0.005680(2) \quad [46],$$

which agrees perfectly with Ref. [46]. These results have also been checked by Taniguchi and Ukawa [47]. We also obtain

$$b_V^{[1]} - b_A^{[1]} = C_F \times 0.0007833(11) = 0.0010444(16) \tag{4.22}$$

by subtracting the integrands first, and then integrating. In taking the difference, large contributions from the self energy cancel, but, even so, the near equality of $b_V^{[1]}$ and $b_A^{[1]}$ is a bit astonishing. Comparing the slopes of Figs. 2(a) and 3(b) one sees that $b_V^{[1]} - b_A^{[1]}$ for the Wilson action is not so small.

Although these checks are reassuring, the main result of this section is to obtain the full mass dependence of the matching factors. The results at intermediate mass, with $m_1 a < 3$ or, equivalently, $m_0 a < 1.5$, are needed for realistic calculations of B meson properties. This region is neither particularly close to the massless limit, nor to the logarithmic behavior of the static limit.

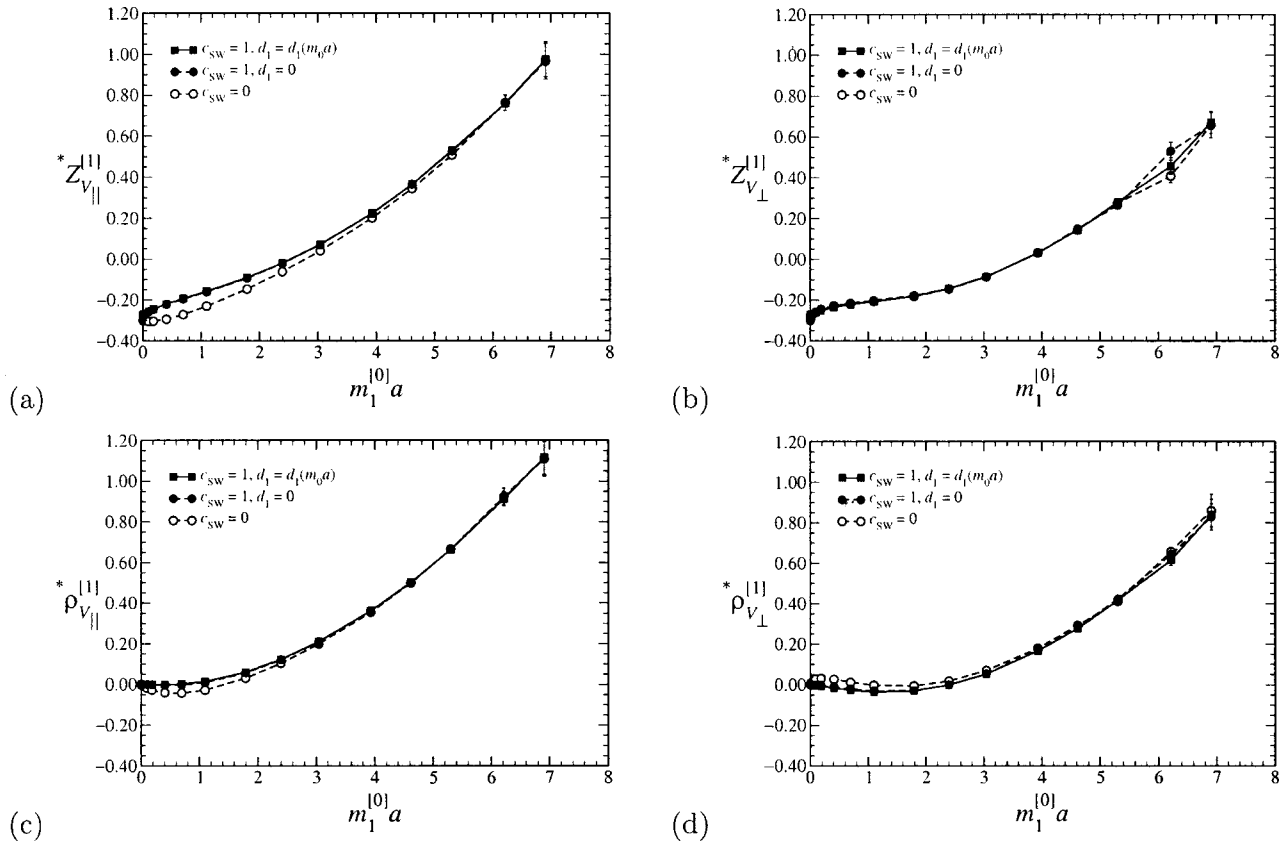

FIG. 4. Full mass dependence of the estimated $\beta_0 g^4$ terms of the matching factors of the vector current (a) $^*Z^{[1]}_{V_\parallel}$, (b) $^*Z^{[1]}_{V_\perp}$, (c) $^*\rho^{[1]}_{V_\parallel}$, and (d) $^*\rho^{[1]}_{V_\perp}$.

B. BLM scales q^*

It is well-known that perturbation theory in the bare coupling $g_0^2(1/a)$ converges poorly. Therefore, we calculate the ingredients needed to determine the Brodsky-Lepage-Mackenzie (BLM) scale [48,49]. For a coupling in scheme S, we denote the BLM expansion parameter $g_S^2(q_S^*)$. The BLM scale q_S^* is given by

$$\ln(q_S^* a)^2 = -b_S^{(1)} + \frac{\int d^4k \ln(ka)^2 f(ka)}{\int d^4k f(ka)}, \qquad (4.23)$$

where k is the gluon momentum, and $f(k)$ is the integrand of the quantity of interest, e.g., $\int d^4k f(k) = Z_J^{[1]}$. The constant $b_S^{(1)}$ is the β_0-dependent part of the one-loop conversion from the arbitrary scheme S to the "V scheme," namely

$$\frac{(4\pi)^2}{g_S^2(q)} = \frac{(4\pi)^2}{g_V^2(q)} + \beta_0 b_S^{(1)} + b_S^{(0)} + O(g^2), \qquad (4.24)$$

where for n_f light quarks $\beta_0 = 11 - 2n_f/3$, and $b_S^{(0)}$ is independent of n_f. The V-scheme coupling $g_V^2(q)$ is defined so that the Fourier transform of the heavy-quark potential reads $V(q) = -C_F g_V^2(q)/q^2$. Equation (4.23) shows that the definitions of q^* in Refs. [48] and [49] are identical in the V scheme.

For our matching factors it is straightforward to weight the integrands with $\ln(ka)^2$ to obtain

$$\ln(q_V^* a)^2 = \frac{^*Z^{[1]}}{Z^{[1]}}, \qquad (4.25)$$

because the integration over d^4k has no divergences. The denominators are the one-loop coefficients given above, and the numerators are presented now.

Figure 4 plots the full mass dependence of the numerators for the vector current, (a) $^*Z^{[1]}_{V_\parallel}$, (b) $^*Z^{[1]}_{V_\perp}$, (c) $^*\rho^{[1]}_{V_\parallel}$, and (d) $^*\rho^{[1]}_{V_\perp}$. As before, these numerical results are for the SW action with rotation (solid lines) and also for the SW and Wilson actions without the rotation (dotted lines). Figure 5 plots the full mass dependence of the numerator of Eq. (4.25) for the axial vector current, (a) $^*Z^{[1]}_{A_\parallel}$, (b) $^*Z^{[1]}_{A_\perp}$, (c) $^*\rho^{[1]}_{A_\parallel}$, and (d) $^*\rho^{[1]}_{A_\perp}$. We have carried out several checks on our calculations. Once again, identical numerical results have been obtained with two or more completely independent programs. Also, at $m_b a = 0$ we reproduce the results, for the Wilson action, of Ref. [44].

For $^*Z_J^{[1]}$ and $^*\rho_J^{[1]}$ the limit of large ma also has distinctive features. In that case

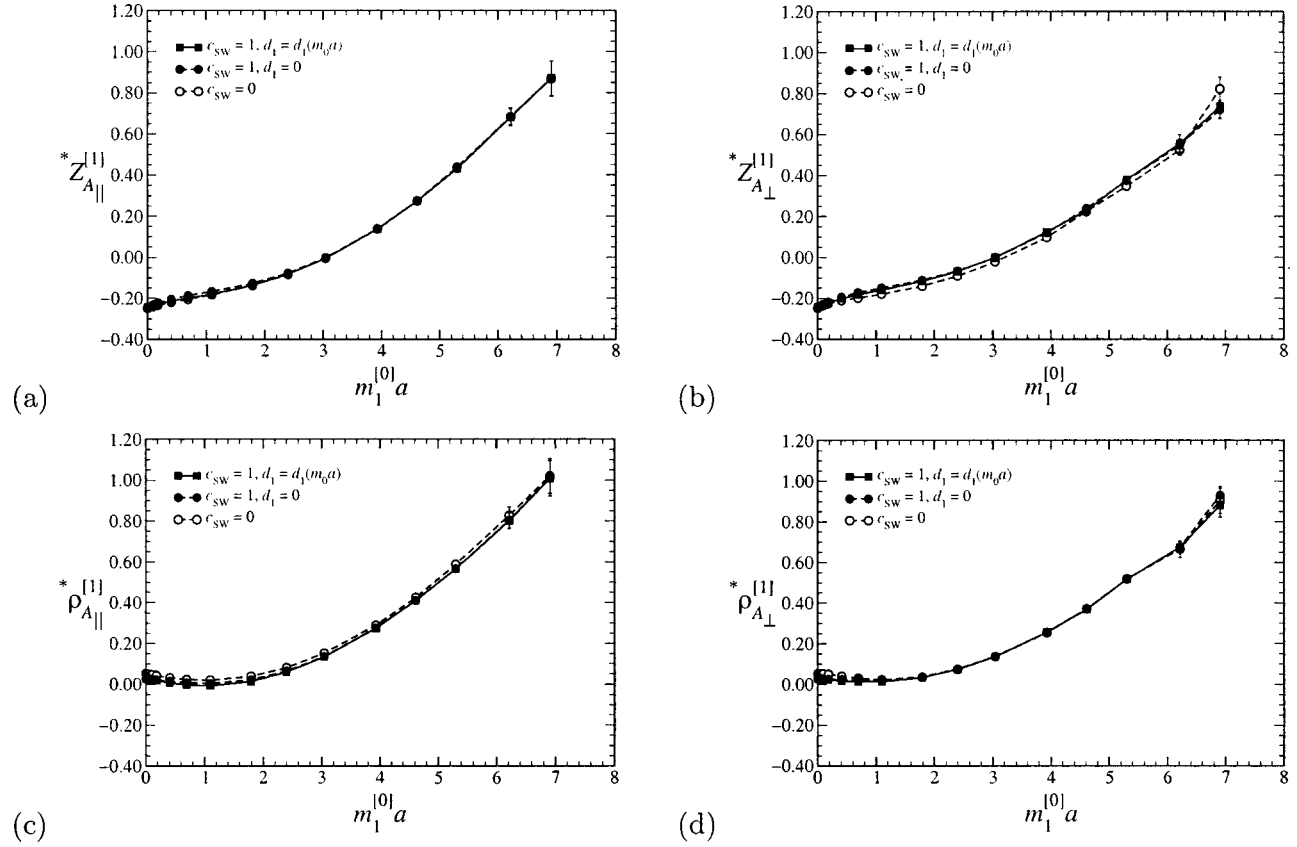

FIG. 5. Full mass dependence of the estimated $\beta_0 g^4$ terms of the matching factors of the axial vector current (a) $^*Z_{A_\parallel}^{[1]}$, (b) $^*Z_{A_\perp}^{[1]}$, (c) $^*\rho_{A_\parallel}^{[1]}$, and (d) $^*\rho_{A_\perp}^{[1]}$.

$$^*Z_J^{[1]}=\frac{C_F}{16\pi^2}[\tfrac{1}{2}\gamma_h \ln^2(m_2a)^2+\gamma_h'\ln(m_2a)^2+{}^*z_J], \tag{4.26}$$

where γ_h' is related to the two-loop anomalous dimension. A similar expression holds for $^*\rho_J^{[1]}$, with a different constant. Note that—in both cases—the one-loop anomalous dimension appears multiplying $\ln^2(m_2a)$. The growth expected from Eq. (4.26) is seen in Figs. 4 and 5. As a consequence, one finds $q^*a\propto\sqrt{m_2a}$ as $ma\to\infty$. Square root behavior is typical of cases with an anomalous dimension.

For the Z factors, the resulting values for q^*a are relatively constant in the ''low mass'' region, $q^*a\sim 2.7$–2.9. Figure 6 shows how q^*a depends on the heavy quark mass in the region $m_1a\leqslant 2$, which is the one most relevant to calculations of decay constants and form factors. At larger masses $Z^{[1]}$ goes through zero, at which point the original BLM prescription breaks down. A prescription for q^* in this case is given in Ref. [50]. For the Wilson action the zero in $Z_{V_\parallel}^{[1]}$ is at a smaller than usual mass [see Fig. 2(a)], which explains its behavior for the BLM q^*a seen in Fig. 6(a). For the ρ factors the denominator $\rho^{[1]}$ is small over most of the interesting region, as seen in Figs. 2(c)–(d) and 3(c)–(d).

It is also interesting to see how q^* changes under tadpole improvement. If one introduces the tadpole-improved matching factors

$$\tilde{Z}_J=Z_J/u_0, \tag{4.27}$$

where the mean link u_0 is any tadpole-dominated short-distance quantity, the arguments of Ref. [49] suggest that the perturbative series for $\tilde{Z}_J$ has smaller coefficients. In analogy with Eq. (4.1) we write

$$e^{-\tilde{m}_1^{[0]}a/2}\tilde{Z}_J=1+\sum_{l=1}^{\infty} g_0^{2l}\tilde{Z}_J^{[l]}, \tag{4.28}$$

where

$$\tilde{m}_1^{[0]}a=\ln[1+m_0a/u_0] \tag{4.29}$$

is the tadpole-improved rest mass. Then

$$\tilde{Z}_J^{[1]}=Z_J^{[1]}-\frac{1}{2}\left(1+\frac{1}{1+m_0a}\right)u_0^{[1]}, \tag{4.30}$$

and because $Z_J^{[1]}<0$ and $u_0^{[1]}<0$ one sees that the one-loop coefficients are reduced. Similarly, for computing the BLM scale

$$^*\tilde{Z}_J^{[1]}={}^*Z_J^{[1]}-\frac{1}{2}\left(1+\frac{1}{1+m_0a}\right)^*u_0^{[1]}. \tag{4.31}$$

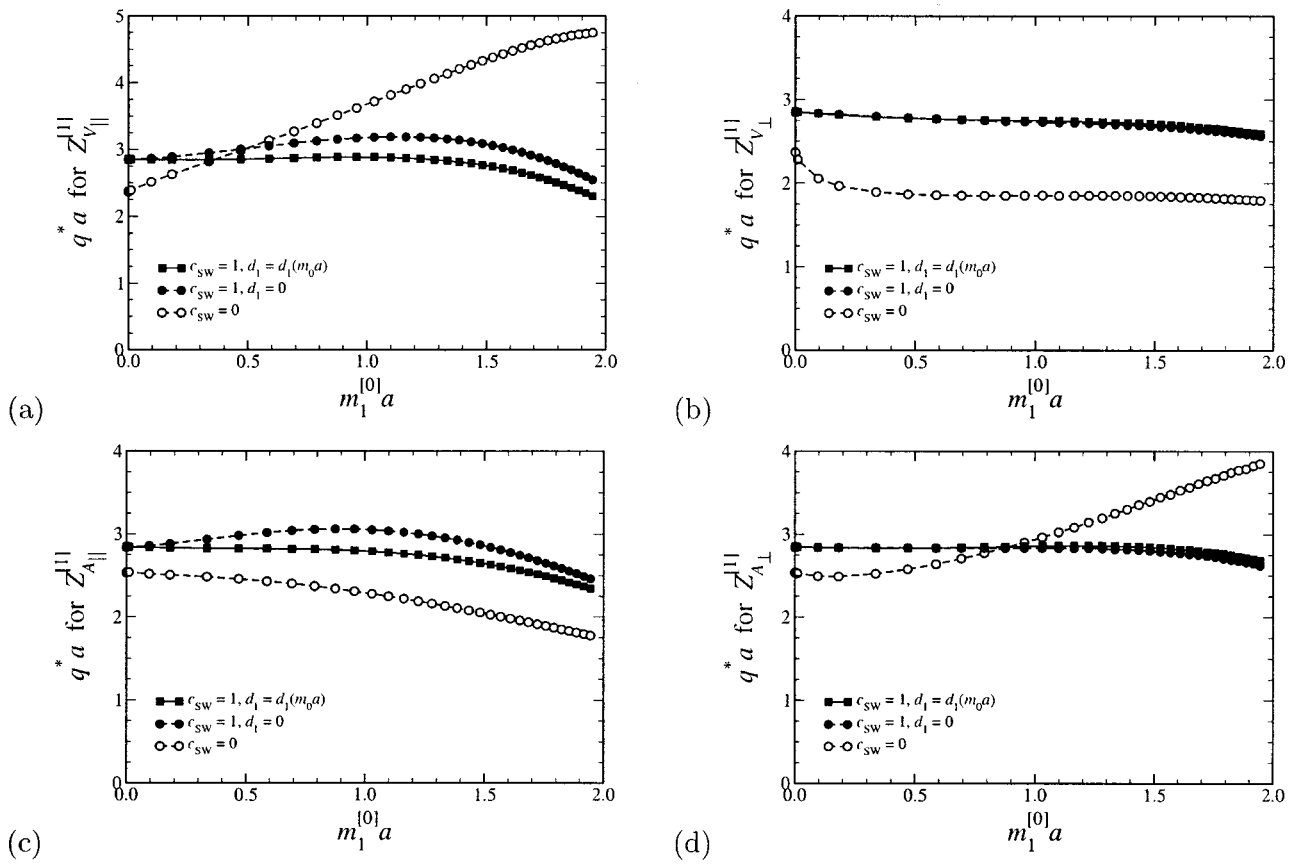

FIG. 6. Full mass dependence of the BLM scale q^*, for (a) $Z_{V_\parallel}$, (b) $Z_{V_\perp}$, (c) $Z_{A_\parallel}$, and (d) $Z_{A_\perp}$.

To illustrate, we take u_0 from the average plaquette, so $u_0^{[1]} = -C_F/16$ and $^*u_0^{[1]} = -0.204049(1)$. Figure 7 shows that, as a rule, q^* is significantly reduced, which means that tadpole improvement has removed some of the most ultraviolet contributions. With a lower scale, the coupling $g_V^2(q^*)$ becomes a bit larger with tadpole improvement. For $Z_{V_\parallel}$ and $Z_{A_\perp}$, however, the denominator $\tilde{Z}_J^{[1]}$ already vanishes for $m_1 a \approx 1.5$–2.0, leading to rapid growth in the BLM q^* for the Wilson action, and a zero in the BLM q^* for the SW action. One should again define q^* in a more robust way [50]. Another choice for the mean field is $u_0 = 8\kappa_{\rm crit}$. It gives coefficients and BLM scales that lie between the unimproved and tadpole-improved cases [51].

Our method also allows us to obtain the BLM scale for the improvement coefficients in the *Alpha* Collaboration's program. Then we are in a position to compare BLM perturbation theory with non-perturbative determinations of these coefficients. We will give these results for q^* and the mentioned comparison in another publication [52].

V. CONCLUSIONS

In this paper we have set up a matching procedure, based on HQET, for heavy-light currents. It is valid for all ma, where m is the heavy quark's mass and a is the lattice spacing, and to all orders in the gauge coupling. It could be applied to lattice NRQCD, although here it is applied to Wilson fermions. In the latter case, HQET matching agrees with Symanzik matching when $ma \ll 1$. In this way, HQET matching is a natural and attractive extension into the regime $ma \not\ll 1$, which is needed for heavy-quark phenomenology.

Our one-loop results for the SW action are of immediate value for lattice calculations of f_B and of form factors for the semi-leptonic decay $B \to \pi l \nu$. Indeed, our earlier one-loop results [12] (which omitted the ''rotation'' terms in the current) were used for f_B in Refs. [19–23], and our results were used for semi-leptonic form factors in Ref. [15]. In particular, we have obtained the BLM scale q^* for the matching factors, which should reduce the uncertainty of one-loop calculations. Similarly, computing part of the normalization factor, namely $\sqrt{Z_{V_\parallel}^{qq} Z_{V_\parallel}^{bb}}$, non-perturbatively reduces the normalization uncertainty even further [13–15]. (The heavy-heavy normalization factor $Z_{V_\parallel}^{bb}$ is defined in our companion paper for heavy-heavy currents [6].)

An outstanding problem at this time is the one-loop calculation of the coefficients $B_{Ji}^{\rm lat}$ of the dimension-four terms in the HQET description. A calculation of these coefficients, and the subsequent adjustment of the parameters b_{Ji} in the lattice currents, would eliminate uncertainties of order $\alpha_s \bar{\Lambda}/m$ and $\alpha_s \bar{\Lambda} a$ in (future) calculations of heavy-quark matrix elements. The algebra quickly becomes voluminous, making this problem well-suited to automated techniques [53].

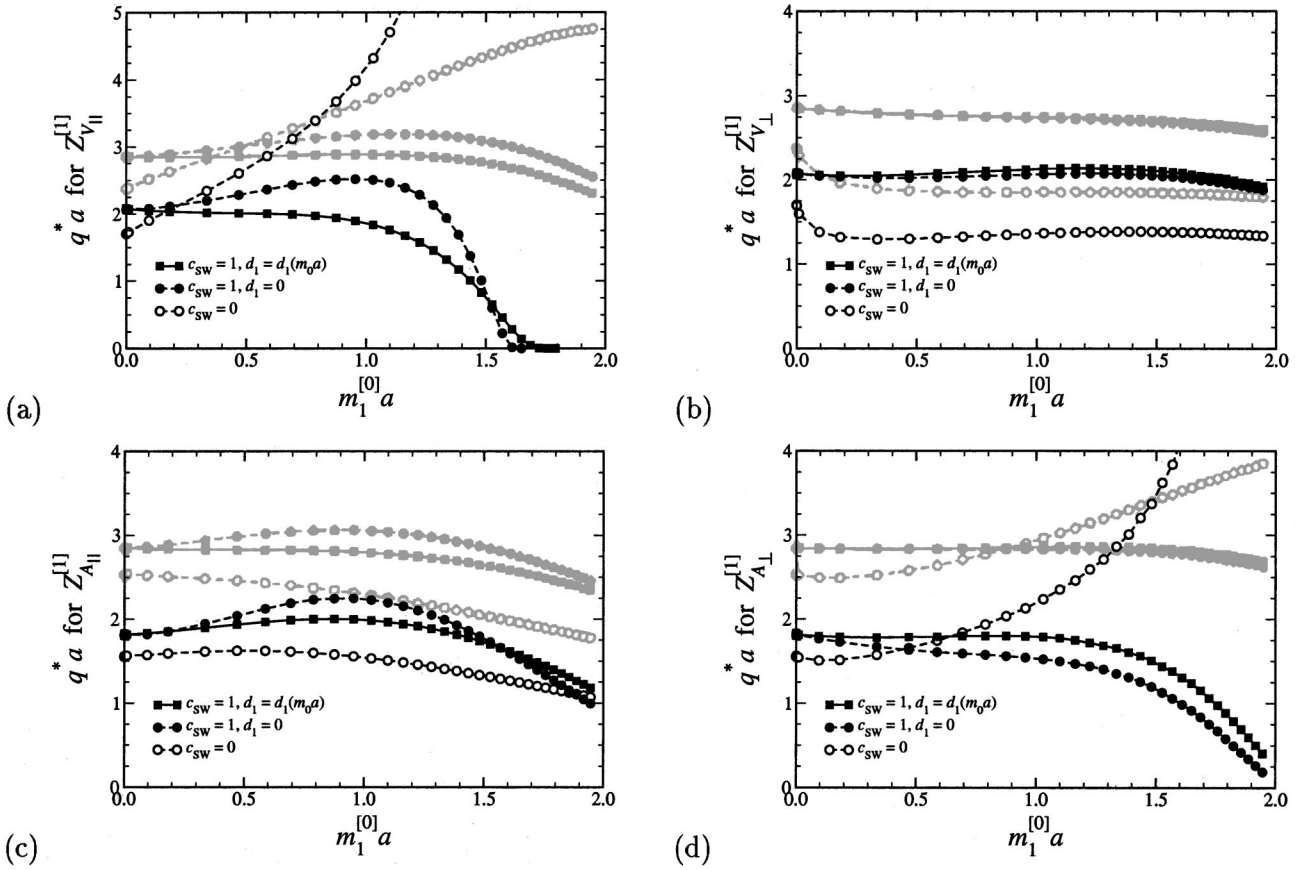

FIG. 7. Tadpole-improved q^* for (a) $\tilde{Z}_{V_\parallel}$, (b) $\tilde{Z}_{V_\perp}$, (c) $\tilde{Z}_{A_\parallel}$, and (d) $\tilde{Z}_{A_\perp}$, with Fig. 6 in gray.

ACKNOWLEDGMENTS

A.S.K. would like to thank Akira Ukawa and the Center for Computational Physics for hospitality while part of this work was being carried out, and the Aspen Center for Physics for a stimulating atmosphere while part of the paper was being written. S.H., A.S.K., and T.O. would also like to thank the Institute for Nuclear Theory at the University of Washington for hospitality while this paper was being finished. S.H. and T.O. are supported by Grants-in-Aid of the Japanese Ministry of Education (Nos. 11740162 and 12640279, respectively). K.-I.I. and N.Y. are supported by the JSPS. Fermilab is operated by Universities Research Association Inc., under contract with the U.S. Department of Energy.

APPENDIX A: FEYNMAN RULES

The needed propagators and vertices for quark-gluon interactions are given in Ref. [31]. Here we give the additional Feynman rules induced by the rotation term of the heavy quark. The additional rules are easy to derive by expressing the covariant difference operator as [54]

$$D^{\mu}_{\rm lat} = [T_{+\mu} - T_{-\mu}]/(2a), \tag{A1}$$

where

$$T_{\pm\mu} = t_{\pm\mu/2} e^{\pm g_0 a A_\mu} t_{\pm\mu/2}, \tag{A2}$$

and $t_{\pm\mu/2}$ translates fields to its right by one-half lattice spacing in the $\pm\mu$ direction.

There are three rules to give, with 0, 1, and 2 gluons emerging from the vertex. Let the Dirac matrix of the current be Γ. Then,

$$0\text{-gluon} = \Gamma\left[1 + i d_1 \sum_r \gamma_r \sin(p_r)\right], \tag{A3}$$

$$1\text{-gluon} = g_0 t^a d_1 \Gamma \gamma_i \cos(p + \tfrac{1}{2}k)_i, \tag{A4}$$

$$2\text{-gluon} = i g_0^2 \tfrac{1}{2}\{t^a, t^b\} \delta_{ij} d_1 \Gamma \gamma_i \sin(p + \tfrac{1}{2}k + \tfrac{1}{2}l)_i, \tag{A5}$$

where momentum p is quark momentum flowing into the vertex, and k and l are gluon momentum flowing into the vertex. As in Ref. [31], the matrices t^a are anti-Hermitian, i.e., $U_\mu = \exp(g_0 t^a A^a_\mu)$, $\Sigma_{aj} t^a_{ij} t^a_{jk} = -C_F \delta_{ik}$, and $\mathrm{tr} t^a t^b = -\frac{1}{2}\delta^{ab}$.

APPENDIX B: DIRAC ALGEBRA

To compute the vertex function, there are four diagrams to consider, depicted in Fig. 8: the usual vertex diagram (with the rotation inside), Fig. 8(a); two diagrams with the gluon connected to the incoming rotation, Fig. 8(b) and (c); and a tadpole diagram connected to the incoming rotation [using rule (A5)], Fig. 8(d). The tadpole diagram, Fig. 8(d), van-

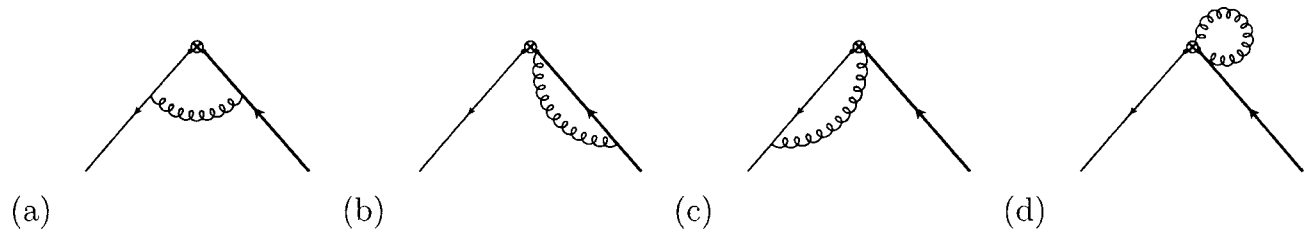

FIG. 8. Feynman diagrams for calculating the vertex function. The ● on each side of the ⊗ indicates the rotation.

ishes for zero external three-momentum, because $l=-k$ and $p_i=0$.

For each non-vanishing diagram, Figs. 8(a–c), define the integral

$$I_\Gamma^{(\mathrm{a,b,c})}=-g_0^2 C_F\int\frac{d^4k}{(2\pi)^4}\frac{1}{\hat{k}^2}\mathcal{I}_\Gamma^{(\mathrm{a,b,c})}, \tag{B1}$$

where k is the momentum of the gluon in the loop, and $\hat{k}_\mu=2\sin(\frac{1}{2}k_\mu)$. Let the incoming massive quark have couplings m_0, r_s, ζ, c_B, and c_E, and external momentum p. Similarly, let the outgoing massless quark have couplings $m_0'=0$, r_s', ζ', c_B', and c_E', and external momentum p'. The internal quark lines carry momentum $p+k$ in and $p'+k$ out. The integrals I are obtained directly from the loop diagrams. Then

$$Z_J^{[1]}=\frac{1}{2}(Z_{2h\,\mathrm{cont}}^{[1]}-Z_{2h\,\mathrm{lat}}^{[1]}+Z_{2l\,\mathrm{cont}}^{[1]}-Z_{2l\,\mathrm{lat}}^{[1]})$$

$$+\sum_{\mathrm{d}}(I_{\Gamma\,\mathrm{cont}}^{\mathrm{d}}-I_{\Gamma\,\mathrm{lat}}^{\mathrm{d}}), \tag{B2}$$

from Eq. (4.1). The relation between the current J and its Dirac matrix Γ is contained in Table I. The expression relating $Z_2^{[1]}{}_{\mathrm{lat}}$ to lattice self-energy functions is in Ref. [31].

The most onerous task in evaluating the diagrams is the manipulation of the Dirac matrices. A convenient method is to treat each quark line separately, starting from the initial-or final-state spinor. Then the spinor, the propagator, and the vertices can be written out in 2×2 block diagonal form, with Pauli matrices appearing in the blocks. Once the Feynman rules are as complicated as in the present calculation, it is easier to manipulate 2×2 matrices of Pauli matrices than to manipulate Dirac matrices. A special advantage of this organization is that the rotation bracket in Eq. (A3) merely ''rotates'' the rest of the leg. We also obtain $Z_2^{[1]}{}_{\mathrm{lat}}$ in this way, with much less effort than in Ref. [31].

A further advantage is that the vertex corrections can be expressed compactly. The diagram with a gluon going from the incoming leg to the rotation, Fig. 8(b), is

TABLE I. The factor s_Γ, defined by $\frac{1}{3}\Sigma_r\gamma_r\Gamma\gamma_r=s_\Gamma\Gamma$.

J	Γ	s_Γ
V_4	γ_4	-1
A_4	$\gamma_4\gamma_5$	$+1$
V_j	γ_j	$-\frac{1}{3}$
A_j	$\gamma_j\gamma_5$	$+\frac{1}{3}$

$$\mathcal{I}_\Gamma^{(\mathrm{b})}=d_1\frac{\zeta}{D}\left[(3-\tfrac{1}{4}\hat{\boldsymbol{k}}^2)L+\tfrac{1}{2}\zeta\sum_r K_r S_r^2\right], \tag{B3}$$

where $S_r=\sin k_r$, and the functions D, L, and K_r are given in Appendix C. The diagram with a gluon going from the outgoing leg to the rotation, Fig. 8(c), is

$$\mathcal{I}_\Gamma^{(\mathrm{c})}=s_\Gamma d_1\frac{\zeta'}{D'}\left[(3-\tfrac{1}{4}\hat{\boldsymbol{k}}^2)\overset{(-)}{L}{}'+\tfrac{1}{2}\zeta'\sum_r K_r' S_r^2\right], \tag{B4}$$

where the functions D', $\overset{(-)}{L}{}'$, and K_r' are given in Appendix C, and s_Γ is given in Table I. The unbarred function L (barred function $\overline{L}$) is for $\Gamma=\gamma_4$ and $\gamma_j\gamma_5$ ($\Gamma=\gamma_j$ and $\gamma_4\gamma_5$).

The vertex diagram, Fig. 8(a), is complicated. We find $\mathcal{I}_\Gamma^{(\mathrm{a})}=N_\Gamma^{(\mathrm{a})}/DD'$, with numerator

$$N_\Gamma^{(\mathrm{a})}=(\pm)(\overset{(-)}{U}{}_0'\mathcal{R}[U_0]-s_\Gamma\overset{(-)}{L}{}_0'\mathcal{R}[L_0]\boldsymbol{S}^2)-\zeta\zeta' X_\Gamma. \tag{B5}$$

The upper sign and unbarred functions (lower sign and barred functions) are for $\Gamma=\gamma_4$ and $\gamma_j\gamma_5$ ($\Gamma=\gamma_j$ and $\gamma_4\gamma_5$). The part X_Γ comes from spatial gluon exchange:

$$X_\Gamma=-s_\Gamma(3-\tfrac{1}{4}\hat{\boldsymbol{k}}^2)\overset{(-)}{L}{}'\mathcal{R}[L]+s_\Gamma^2(3-\tfrac{1}{4}\hat{\boldsymbol{k}}^2)\overset{(-)}{V}{}'\mathcal{R}[V]\boldsymbol{S}^2$$

$$+\tfrac{1}{2}(\overset{(-)}{V}{}'\mathcal{R}[U]-s_\Gamma\overset{(-)}{L}{}'\mathcal{R}[\zeta])\sum_r K_r S_r^2$$

$$+\tfrac{1}{2}(\overset{(-)}{U}{}'\mathcal{R}[V]-s_\Gamma\zeta'\mathcal{R}[L])\sum_r K_r' S_r^2$$

$$+\tfrac{1}{4}(\overset{(-)}{U}{}'\mathcal{R}[U]-s_\Gamma\boldsymbol{S}^2\zeta'\mathcal{R}[\zeta])\sum_r K_r' K_r\hat{k}_r^2+\tfrac{1}{8}(1-s_\Gamma^2)$$

$$\times\left(\hat{\boldsymbol{k}}^2\boldsymbol{S}^2-3\sum_r\hat{k}_r^2 S_r^2\right)\overset{(-)}{V}{}'\mathcal{R}[V], \tag{B6}$$

where the last term is absent for V_4 and A_4 (i.e., when $s_\Gamma^2=1$). The rotation enters in the ''rotated'' functions

$$\mathcal{R}[U_0]=U_0+d_1\boldsymbol{S}^2L_0, \tag{B7}$$

$$\mathcal{R}[L_0]=L_0-d_1U_0, \tag{B8}$$

$$\mathcal{R}[U]=U+d_1\boldsymbol{S}^2\zeta, \tag{B9}$$

$$\mathcal{R}[\zeta]=\zeta-d_1U, \tag{B10}$$

$$\mathcal{R}[V]=V+d_1L, \tag{B11}$$

$$\mathcal{R}[L]=L-d_1\boldsymbol{S}^2V. \tag{B12}$$

Although the vertex diagram is not easy to write down, the rotation modifies it in a fairly simple way, when using the 2×2 Pauli matrix method described above.

We have verified that these expressions are correct by completely independent calculation with more common methods for the Dirac algebra.

APPENDIX C: USEFUL FUNCTIONS

In this appendix we list the functions appearing in Appendix B for the action and currents given in Sec. III. First, let

$$\mu=1+m_0+\tfrac{1}{2}r_s\zeta\hat{\boldsymbol{k}}^2, \tag{C1}$$

$$\mu'=1+m_0'+\tfrac{1}{2}r_s'\zeta'\hat{\boldsymbol{k}}^2. \tag{C2}$$

From now on a prime means to replace incoming couplings and momenta with corresponding outgoing couplings and momenta.

When the quark propagator is rationalized it has the denominator

$$D=1-2\mu\cos(k_4+im_1^{[0]})+\mu^2+\zeta^2\boldsymbol{S}^2, \tag{C3}$$

where $m_1^{[0]}=\ln(1+m_0)$.

In this calculation, the heavy quark has zero three-momentum, so its spinor consists only of upper components. Depending on the matrix Γ the heavy quark couples either to the upper or lower components of the light quark. With the upper components the unbarred functions arise, and with the lower components (of the light quark) the barred functions arise.

To express the useful functions compactly, it is convenient to introduce first

$$U=\mu-e^{-m_1^{[0]}+ik_4}, \tag{C4}$$

$$\overline{U}=\mu-e^{+m_1^{[0]}-ik_4}, \tag{C5}$$

because these combinations appear in the other functions. Then

$$U_0=Ue^{+m_1^{[0]}-ik_4/2}-\tfrac{1}{2}\zeta^2c_E\cos(\tfrac{1}{2}k_4)\boldsymbol{S}^2, \tag{C6}$$

$$L_0=\zeta[e^{+m_1^{[0]}-ik_4/2}+\tfrac{1}{2}c_E\cos(\tfrac{1}{2}k_4)\overline{U}], \tag{C7}$$

$$V=\zeta\left[1+\frac{i}{2}c_E\sin(k_4)\right]+\tfrac{1}{2}c_BU, \tag{C8}$$

$$L=-\overline{U}\left[1+\frac{i}{2}c_E\sin(k_4)\right]+\tfrac{1}{2}c_B\zeta\boldsymbol{S}^2, \tag{C9}$$

$$K_r=r_s-c_B\cos^2(\tfrac{1}{2}k_r)=(r_s-c_B)+\tfrac{1}{4}c_B\hat{k}_r^2, \tag{C10}$$

and

$$\overline{U}_0=\overline{U}e^{-m_1^{[0]}+ik_4/2}-\tfrac{1}{2}\zeta^2c_E\cos(\tfrac{1}{2}k_4)\boldsymbol{S}^2, \tag{C11}$$

$$\overline{L}_0=\zeta[e^{-m_1^{[0]}+ik_4/2}+\tfrac{1}{2}c_E\cos(\tfrac{1}{2}k_4)U], \tag{C12}$$

$$\overline{V}=\zeta\left[1-\frac{i}{2}c_E\sin(k_4)\right]+\tfrac{1}{2}c_B\overline{U}, \tag{C13}$$

$$\overline{L}=-U\left[1-\frac{i}{2}c_E\sin(k_4)\right]+\tfrac{1}{2}c_B\zeta\boldsymbol{S}^2. \tag{C14}$$

The barred functions are obtained from unbarred counterparts by putting $k\rightarrow-k$ and $m_1^{[0]}\rightarrow-m_1^{[0]}$, so there is no need to introduce $\overline{K_r}=K_r$. In the present calculation the barred functions arise only for the outgoing massless quark, for which $m_0'=m_1'^{[0]}=0$.

[1] A.S. Kronfeld and P.B. Mackenzie, Annu. Rev. Nucl. Part. Sci. **43**, 793 (1993); For recent status, see S. Hashimoto, Nucl. Phys. B (Proc. Suppl.) **83**, 3 (2000); S. Aoki, in *Proceedings of the XIX International Symposium on Lepton and Photon Interactions at High Energy*, Stanford, California, 1999, edited by J.A. Jaros and M.E. Peskin [Int. J. Mod. Phys. A **15S1**, 657 (2000)]; S. Ryan, Nucl. Phys. B (Proc. Suppl.) **106**, 86 (2002).

[2] N. Isgur and M.B. Wise, Phys. Lett. B **232**, 113 (1989); **237**, 527 (1990).

[3] W.E. Caswell and G.P. Lepage, Phys. Lett. **167B**, 437 (1986); G.T. Bodwin, E. Braaten, and G.P. Lepage, Phys. Rev. D **46**, 1914 (1992).

[4] A.S. Kronfeld, Phys. Rev. D **62**, 014505 (2000).

[5] A.X. El-Khadra, A.S. Kronfeld, and P.B. Mackenzie, Phys. Rev. D **55**, 3933 (1997).

[6] J. Harada, S. Hashimoto, A.S. Kronfeld, and T. Onogi, following paper, Phys. Rev. D **65**, 094514 (2002); A.S. Kronfeld and S. Hashimoto, Nucl. Phys. B (Proc. Suppl.) **73**, 387 (1999).

[7] K. Symanzik, in *Recent Developments in Gauge Theories*, edited by G. 't Hooft *et al.* (Plenum, New York, 1980).

[8] K. Symanzik, in *Mathematical Problems in Theoretical Physics*, edited by R. Schrader *et al.* (Springer, New York, 1982); Nucl. Phys. **B226**, 187 (1983).

[9] M. Lüscher, S. Sint, R. Sommer, and P. Weisz, Nucl. Phys. **B478**, 365 (1996).

[10] K. Jansen *et al.*, Phys. Lett. B **372**, 275 (1996); M. Lüscher, S. Sint, R. Sommer, P. Weisz, and U. Wolff, Nucl. Phys. **B491**, 323 (1997).

[11] Y. Kuramashi, Phys. Rev. D **58**, 034507 (1998).

[12] K.-I. Ishikawa *et al.*, Nucl. Phys. B (Proc. Suppl.) **63**, 344 (1998); K.-I. Ishikawa, T. Onogi, and N. Yamada, *ibid.* **83**, 301 (2000).

[13] S. Hashimoto *et al.*, Phys. Rev. D **61**, 014502 (2000).

[14] J.N. Simone *et al.*, Nucl. Phys. B (Proc. Suppl.) **83**, 334 (2000); S. Hashimoto *et al.*, hep-ph/0110253.

[15] A.X. El-Khadra, A.S. Kronfeld, P.B. Mackenzie, S.M. Ryan,

and J.N. Simone, Phys. Rev. D **64**, 014502 (2001).
[16] B. Sheikholeslami and R. Wohlert, Nucl. Phys. **B259**, 572 (1985).
[17] K.G. Wilson, in *New Phenomena in Subnuclear Physics*, edited by A. Zichichi (Plenum, New York, 1977).
[18] A.S. Kronfeld, Nucl. Phys. B (Proc. Suppl.) **42**, 415 (1995).
[19] JLQCD Collaboration, S. Aoki *et al.*, Phys. Rev. Lett. **80**, 5711 (1998).
[20] A.X. El-Khadra *et al.*, Phys. Rev. D **58**, 014506 (1998).
[21] C. Bernard *et al.*, Phys. Rev. Lett. **81**, 4812 (1998).
[22] CP-PACS Collaboration, A. Ali Khan *et al.*, Nucl. Phys. B (Proc. Suppl.) **83**, 331 (2000); Phys. Rev. D **64**, 034505 (2001).
[23] MILC Collaboration, C. Bernard *et al.*, Nucl. Phys. B (Proc. Suppl.) **83**, 289 (2000); **94**, 346 (2001).
[24] J. Harada, A.S. Kronfeld, H. Matsufuru, N. Nakajima, and T. Onogi, Phys. Rev. D **64**, 074501 (2001).
[25] G.P. Lepage and B.A. Thacker, Nucl. Phys. B (Proc. Suppl.) **4**, 199 (1987); B.A. Thacker and G.P. Lepage, Phys. Rev. D **43**, 196 (1991); G.P. Lepage, L. Magnea, C. Nakhleh, U. Magnea, and K. Hornbostel, *ibid.* **46**, 4052 (1992).
[26] E. Eichten, Nucl. Phys. B (Proc. Suppl.) **4**, 170 (1987).
[27] E. Eichten and B. Hill, Phys. Lett. B **234**, 511 (1990); **240**, 193 (1990).
[28] C.T.H. Davies and B.A. Thacker, Phys. Rev. D **48**, 1329 (1993).
[29] C.J. Morningstar and J. Shigemitsu, Phys. Rev. D **57**, 6741 (1998); **59**, 094504 (1999).
[30] For the program, see http://theory.fnal. gov/people/kronfeld/LatHQ2QCD/or the EPAPS Document accompanying this paper and Ref. [6]. See EPAPS Document No. E-PRVDAQ-65-042209 for a suite of programs, including programs that calculate the one-loop matching factor of heavy-heavy and heavy-light currents for Fermilab actions of lattice heavy quarks. This document may be retrieved via the EPAPS homepage (http://www.aip.org/pubservs/epaps.html) or from ftp.aip.org in the directory /epaps/. See the EPAPS homepage for more information.
[31] B.P.G. Mertens, A.S. Kronfeld, and A.X. El-Khadra, Phys. Rev. D **58**, 034505 (1998).
[32] A.F. Falk, M. Neubert, and M. Luke, Nucl. Phys. **B388**, 363 (1992).
[33] R. Wohlert, DESY report DESY 87/069.
[34] B. Grinstein, Nucl. Phys. **B339**, 253 (1990).
[35] H. Georgi, Phys. Lett. B **240**, 447 (1990).
[36] E. Eichten and B. Hill, Phys. Lett. B **243**, 427 (1990).
[37] M. Luke and A.V. Manohar, Phys. Lett. B **286**, 348 (1992); M. Neubert, *ibid.* **306**, 357 (1993); R. Sundrum, Phys. Rev. D **57**, 331 (1998).
[38] T.L. Trueman, Z. Phys. C **69**, 525 (1996).
[39] A.S. Kronfeld, Phys. Rev. D **58**, 051501 (1998).
[40] E. Gabrielli *et al.*, Nucl. Phys. **B362**, 475 (1991).
[41] M. Lüscher, S. Sint, R. Sommer, and H. Wittig, Nucl. Phys. **B491**, 344 (1997).
[42] S. Capitani *et al.*, Nucl. Phys. **B593**, 183 (2001).
[43] G. Martinelli and Y. Zhang, Phys. Lett. **123B**, 433 (1983).
[44] C. Bernard, M. Golterman, and C. McNeile, Phys. Rev. D **59**, 074506 (1999).
[45] A. Borrelli and C. Pittori, Nucl. Phys. **B385**, 502 (1992).
[46] S. Sint and P. Weisz, Nucl. Phys. **B502**, 251 (1997).
[47] Y. Taniguchi and A. Ukawa, Phys. Rev. D **58**, 114503 (1998).
[48] S.J. Brodsky, G.P. Lepage, and P.B. Mackenzie, Phys. Rev. D **28**, 228 (1983).
[49] G.P. Lepage and P.B. Mackenzie, Phys. Rev. D **48**, 2250 (1993).
[50] K. Hornbostel, G.P. Lepage, and C. Morningstar, Nucl. Phys. B (Proc. Suppl.) **94**, 579 (2001).
[51] J. Harada *et al.*, Nucl. Phys. B (Proc. Suppl.) **106**, 802 (2002).
[52] J. Harada, S. Hashimoto, A. S. Kronfeld, and T. Onogi (in preparation).
[53] M. Nobes, H. Trottier, G.P. Lepage, and Q. Mason, Nucl. Phys. B (Proc. Suppl.) **106**, 838 (2002).
[54] A.S. Kronfeld and D.M. Photiadis, Phys. Rev. D **31**, 2939 (1985).

Erratum: Application of heavy-quark effective theory to lattice QCD. II. Radiative corrections to heavy-light currents [Phys. Rev. D 65, 094513 (2002)]

Junpei Harada, Shoji Hashimoto, Ken-Ichi Ishikawa, Andreas S. Kronfeld, Tetsuya Onogi, and Norikazu Yamada

(Received 30 December 2004; published 19 January 2005)

DOI: 10.1103/PhysRevD.71.019903 PACS numbers: 12.38.Gc, 13.20.He, 12.15.Hh, 99.10.Cd

In Ref. [1] the numerical values in Eqs. (4.9) and (4.10) should read

$$z_{A_\perp}^{[1]} = \begin{cases} -12.248, & c_{\mathrm{SW}} = 1, \\ -9.929, & c_{\mathrm{SW}} = 0, \end{cases} \tag{4.9}$$

$$z_{V_\perp}^{[1]} = \begin{cases} -18.414, & c_{\mathrm{SW}} = 1, \\ -24.379, & c_{\mathrm{SW}} = 0, \end{cases} \tag{4.10}$$

These values are consistent with the asymptotic behavior exhibited in Figs. 2 and 3.

Our calculations in the static limit were described in Ref. [2], which should have been cited at the end of the sentence following Eq. (4.10).

We thank Matthew Nobes for detecting the error.

[1] J. Harada, S. Hashimoto, K. I. Ishikawa, A. S. Kronfeld, T. Onogi, and N. Yamada, Phys. Rev. D **65**, 094513 (2002).

[2] K. I. Ishikawa, T. Onogi, and N. Yamada, Phys. Rev. D **60**, 034501 (1999).

